arXiv:nucl-th/0306044v4 5 Sep 2003

Transparent Nuclei and Deuteron-Gold Collisions at RHIC*

B.Z. Kopeliovich

Max-Planck Institut für Kernphysik, Postfach 103980, 69029 Heidelberg

Institut für Theoretische Physik der Universität, 93040 Regensburg

Joint Institute for Nuclear Research, Dubna, 141980 Moscow Region, Russia

Abstract

The current normalization of the cross section of inclusive high-p_T particle production in deuteron-gold collisions measured at RHIC relies on Glauber model calculations for the inelastic dAu cross section. These calculations should be corrected for diffraction. Moreover, they miss the Gribov's inelastic shadowing which makes nuclei more transparent (color transparency) and reduce the inelastic cross section. The magnitude of this effect rises with energy and one may anticipate it to affect dramatically the normalization of the RHIC data. We evaluate the inelastic shadowing corrections employing the light-cone dipole formalism which effectively sums up multiple interactions in all orders. We found a rather modest correction factor for the current normalization of data for high-p_T hadron production in $d-Au$ collisions. The results of experiments insensitive to diffraction (PHENIX, PHOBOS) should be renormalized by about 20% down, while those which include diffraction (STAR), by only 10%. In spite of smallness of the correction it eliminates the Cronin enhancement in the PHENIX data for pions. The largest theoretical uncertainty comes from the part of inelastic shadowing which is related to diffractive gluon radiation, or gluon shadowing. Our estimate is adjusted to data for the triple-Pomeron coupling and is small, however, other models do not have such a restrictions and predict much stronger gluon shadowing. Thus, one arrives at quite diverse predictions for the correction factor which may be even as small as $K = 0.65$. Therefore, one should admit that the current data for high-p_T hadron production in dAu collisions at RHIC cannot exclude in a model independent way a possibility of initial state suppression proposed by Kharzeev-Levin-McLerran. To settle this uncertainty one should directly measure of the inelastic $d-Au$ cross sections at RHIC. Also collisions with a tagged spectator nucleon may serve as a sensitive probe for nuclear transparency and inelastic shadowing. We found an illuminating quantum-mechanical effect: the nucleus acts like a lens focusing spectators into a very narrow cone.

*Based on lectures given by the author at Workshop on High p_T Correlations at RHIC, Columbia University, May-June, 2003.

Contents

1 Introduction **3**
- 1.1 Number of collisions: who is actually colliding? . . . 3
- 1.2 Correcting data for R_{d-Au} . . . 5
  - 1.2.1 Inelastic shadowing. . . . 5
  - 1.2.2 How inelastic is the inelastic cross section? . . . 6
- 1.3 The outline . . . 7

2 Extending the Glauber model to deuteron-nucleus collisions **8**
- 2.1 The total cross section . . . 9
- 2.2 The cross section of elastic dA scattering and deuteron breakup $dA \to pnA$ 9
- 2.3 The total inelastic cross section . . . 11
- 2.4 The cross section of nondiffractive channels . . . 11

3 Quantum mechanics at work: illuminating focusing effect for spectators **13**

4 Inelastic shadowing corrections **20**
- 4.1 Intermediate state diffractive excitations . . . 20
- 4.2 Eigenstate method . . . 21

5 Light-cone dipoles and inelastic shadowing **23**
- 5.1 Excitation of the valence quark skeleton . . . 23
  - 5.1.1 Nuclear transparency . . . 24
  - 5.1.2 Cross sections . . . 24
- 5.2 Deuteron-nucleus collisions . . . 26
- 5.3 Towards realistic calculations . . . 28
  - 5.3.1 Three valence quarks . . . 28
  - 5.3.2 Realistic dipole cross section . . . 29

6 Gluon shadowing and the triple-Pomeron diffraction **31**
- 6.1 The Green function for glue-glue dipoles . . . 31
- 6.2 More models for gluon shadowing . . . 36
- 6.3 Number of participants . . . 37

7 Cronin effect: renormalizing the data **37**

8 Summary and conclusions **40**

9 Appendix **42**
- A Glauber model glossary . . . 42
  - A.1 Heavy nuclei . . . 43
  - A.2 Proton-deuteron collisions . . . 44
- B Deuteron wave function at rest and Lorentz boosted . . . 46

1 Introduction

Recent data for high-p_T hadron production in deuteron-gold collisions at $\sqrt{s} = 200\,\mathrm{GeV}$ at RHIC [1–3] demonstrate importance of these measurements for proper interpretation of data from heavy ion collisions. The observed nuclear effects at high-p_T are pretty weak, the enhancement (Cronin effect) measured for pions by PHENIX is only about $10 - 20\%$, in accordance with expectation of [4] and with somewhat larger effect found in [5], while a suppression, rather than enhancement was predicted in [6]. To discriminate between these predictions the data should have at least few percent accuracy.

In this notes we draw attention to the fact that only the shape of p_T-distribution was measured experimentally, while the normalization of the data is based on theoretical calculations which are not correct. Therefore, the reported results of deuteron-gold measurements [1–3] may be altered by more appropriate calculations.

The nucleus to nucleon ratio demonstrating the well known Cronin effect [7] is defined as,

$$R_{A/N}(p_T) = \frac{d\sigma^{hA}/d^2p_T}{A\, d\sigma^{hN}/d^2p_T}\ . \tag{1}$$

At large p_T, of the order of few GeV this ratio exceeds one, but eventually approaches one at very high p_T as is expected according to k_T-factorization (it may even drop below one due to the EMC effect at large Bjorken x).

Absolute values of the high-p_T nuclear cross sections are difficult to measure at RHIC, only the fraction of the total inelastic cross section, dN^{hA}/d^2p_T is known. Then, one has to normalize it multiplying the fraction by the total inelastic cross section,

$$R_{A/N}(p_T) = \frac{\sigma_{in}^{hA}\, dN^{hA}/d^2p_T}{A\,\sigma_{in}^{NN}\, dN^{hN}/d^2p_T} = \frac{1}{N_{coll}}\ \frac{dN^{hA}/d^2p_T}{dN^{hN}/d^2p_T}\ , \tag{2}$$

where

$$N_{coll} = A\,\frac{\sigma_{in}^{hN}}{\sigma_{in}^{hA}}\ , \tag{3}$$

In some experiments the denominator in (1), $d\sigma^{hN}/d^2p_T$ was directly measured or borrowed from other measurements, otherwise it should be corrected for diffractive dissociation of the colliding protons which possesses a large rapidity gap and escapes detection. In what follows we assume that the denominator in (1), $d\sigma^{hN}/d^2p_T$ was directly measured (see, however, discussion in Sect. 1.2.2) and concentrate on nuclear effects, i.e. the inelastic nuclear cross section σ_{in}^{NA} which was calculated in [1–3] in an oversimplified approach.

1.1 Number of collisions: who is actually colliding?

The Glauber approach is a model for the elastic hadron-nucleus amplitude. It is demonstrated in Appendix A how to calculate inelastic and quasielastic cross section using unitarity and completeness. The model does not say anything about exclusive channels of inelastic interaction. One can formally expand the Glauber exponential, and it looks like a series corresponding to different numbers of inelastic collisions of the same hadron and with the

same inelastic cross section. However, a high-energy hadron cannot interact inelastically many times, since the very first inelastic collision breaks down coherence between the constituents of the hadron. It takes a long time proportional to the energy to produce a leading hadron in final state.

The cross section of inelastic hadron-nucleus collision, σ_{in}^{hA}, is related to the probability for the incoming hadron to get the very first inelastic collision, usually on the nuclear surface. This is why $\sigma_{in}^{hA} \propto A^{2/3}$. Since the process is fully inclusive, subsequent final state interactions do not affect the cross section due to completeness.

N_{coll} defined via expansion of the Glauber exponential term should not be treated as multiple sequential interactions of the projectile hadron (like expansion of the exponential describing the time dependence of particle decay does not mean that the particle can decay many times). After the first inelastic interaction the debris of the projectile hadron keep traveling through the nucleus, but their interactions apparently have little to do with the properties of the incoming hadron and its inelastic cross section. Formally, one can relate N_{coll} to the mean number of the Pomerons which undergo unitarity cuts. The Abramovsky-Gribov-Kancheli (AGK) cutting rules [8] which are not proven in QCD, assume that these cuts have the same eikonal weights as given by the Glauber model. In this approach multiple interactions are not sequential (planar), but occur in parallel, i.e. they allow a simultaneous unitarity cut. In terms of the light-cone approach multiple interactions correspond to higher Fock states in the projectile hadron. The constituents of this states propagate through the nucleus and experience their first inelastic interactions independently of each other. The probability of such multiple interactions has little to do with the properties of the low Fock states which dominate the hadron-nucleon cross section, therefore it should not be expressed as a power of σ_{in}^{hN}. At any rate, whether the AGK weights are correct or not, it is clear N_{coll} cannot be treated as sequential interactions of the projectile hadron.

The first inelastic collision of the incoming hadron is a soft color-exchange interaction. The projectile partons do not alter either their number (for a given Fock state), or their longitudinal momenta, but the whole system of partons acquire a color. Therefore, the remnants of the hadron turn out to be color connected to the remnants of the target. Then new partons are produced from vacuum (e.g. via the Schwinger mechanism) aiming to neutralize the color of the projectile partons. Their momenta are much smaller than of the projectile partons. Such an excited and color neutral partonic system keeps propagating through the medium and experiencing new soft color exchange interactions similar to ordinary hadrons. The corresponding cross section is subject to color screening and is controlled by the transverse, rather than longitudinal size of the system.

From the practical point of view, there is nothing wrong in using N_{coll} as a multiplication factor for hard reactions, since within the Glauber model it is proportional to the nuclear thickness function $T_A^N(b)$, i.e. to the number of opportunities for a parton to perform a hard process. Indeed, the projectile high energy partons participate in hard reactions independently of the accompanying partons, since color screening plays no role for a hard interaction. Moreover, naively, one may expect that this factor $T_A^N(b)$ (T_{AB} in the case of AB collision) is all one needs to normalize a hard process, and this normalization is independent of the soft cross section σ_{in}^{hN}. However, N_{coll} is defined for events where inelastic collision did happen. Therefore, it must be properly normalized by the probability for the incoming

hadron to make inelastic interaction at the given impact parameter,

$$N_{coll}(b) = \frac{\sigma_{in}^{NN}\, T_A^N(b)}{1 - \exp[-\sigma_{in}^{NN}\, T_A^N(b)]} \ . \tag{4}$$

Averaging this expression over inelastic collisions at different impact parameters one indeed arrives to the expression Eq. (3).

1.2 Correcting data for R_{d-Au}

The current analyses of RHIC data [1–3] calculate N_{coll} in Glauber Monte Carlo model assuming $\sigma_{in}^{NN} = 41 - 42\,\mathrm{mb}$. In these notes we challenge these calculations and show that the published results for $d - Au$ collisions are subject to important corrections and the conclusions are model dependent.

There are two major corrections to be done to the Cronin ratio Eq. (2) measured at RHIC. We combine them in a correction factor K,

$$R_{dA}(p_T) = R_{dA}^{RHIC}(p_T) \times K \ , \tag{5}$$

where

$$K = K_{Gr} \times K_{Gl} \ . \tag{6}$$

Here K_{Gr} is the correction related to Gribov's inelastic shadowing missed in Glauber model calculations. It is introduced in Sect. 1.2.1 and calculated throughout the paper.

Even within the Glauber model the calculations performed in [1–3] should be corrected by a factor K_{Gl}. It originates from a more accurate treatment of the inelastic NN cross section which should correspond to the class of events selected for the analysis, as is explained in Sect. 1.2.2. This correction is calculated in Sect. 2.

There is an additional correction which should be included into (6) if one needs to compare with theoretical predictions for the Cronin effect for pA collisions. It is related to the fact that the deuteron is a nucleus and is also subject to the Cronin effect. Therefore high-p_T enhancement in $d - A$ must be somewhat stronger than in $p - A$ collisions. This correction is evaluated in Sect. 7 and found rather small.

1.2.1 Inelastic shadowing.

It is known that Gribov's inelastic corrections [9] to the Glauber approximation make nuclear matter more transparent and reduce the hadron-nucleus cross sections compared to the Glauber model. This effect steeply rises with energy, as one can see from the example depicted in Fig. 1 for the total neutron-lead cross section measured and calculated in [10]. Apparently, the Glauber model overestimates the cross section, and the deviation rises with energy. Without a good theoretical input one cannot predict what will happen at the energy of RHIC which is 100 times higher than in fixed-target experiments at Fermilab. This is a serious challenge for the theory to calculate the inelastic dA cross section at these energies, and the results apparently will be model dependent. However, it is certain that the sign of

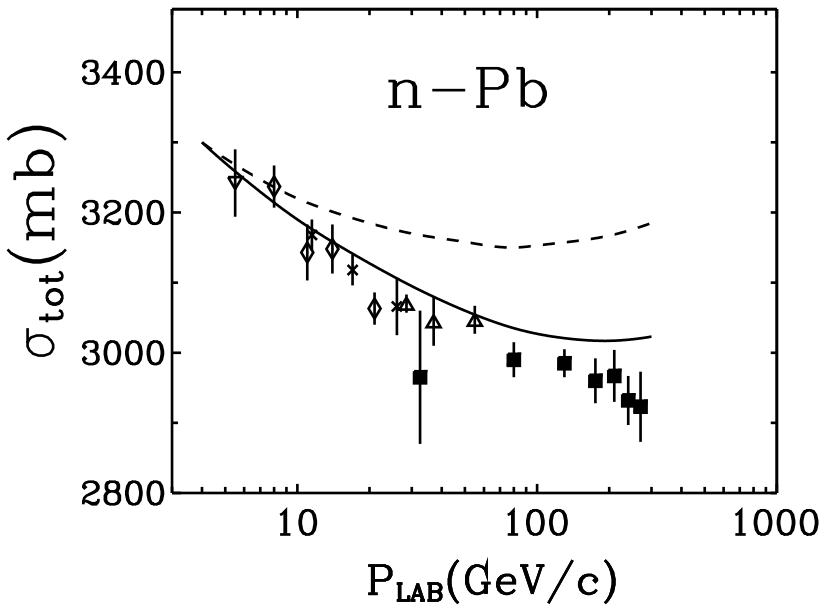

Figure 1: *Data and calculations [10] for the total neutron-lead cross section as function of energy. The dashed curve corresponds to the Glauber model, while the solid curve is corrected for Gribov's inelastic shadowing.*

the correction remains negative and it can only rise with energy, i.e. cannot be smaller than what is shown in Fig. 1 for low energies.

Our own estimates summarized in Table 1 give a moderate reduction, about 20%. The weakness of the effect is based on a proper treatments of diffraction and is fixed by data on large mass diffractive dissociation of protons [11]. At the same time, many models predict quite a strong gluon shadowing even at high virtualities. Naturally, this effect should not be weaker in soft NN interactions. Then it may lead to a stronger suppression of the inelastic dA cross section than we found, as it is discussed in Sect. 6.2.

Note that although inelastic shadowing makes nuclear medium more transparent, the mean number of collisions increases according to (3). It sounds counter-intuitive that a hadron experiences more collisions in a less absorptive medium. Formally it follows from 3), but can be explained qualitatively. For instance, if one calculated the mean number of collisions in a photoabsorption reaction on a nucleus using the Glauber formula, the result will be very small, proportional to α_{em}. However, N_{coll} is defined for events when inelastic collision took place. In this case it comes from hadronic fluctuations of the photon and is much larger than number of collisions given by the Glauber formulas Eq. (3). This example explains why N_{coll} increases due to inelastic shadowing.

1.2.2 How inelastic is the inelastic cross section?

As far as one needs to calculate the deuteron-nucleus inelastic cross section it should be done in correspondence with the class of events selected by the trigger. The cross section

calculated via Glauber Monte-Carlo generator in all three experiments corresponds to the Glauber formula derived in Appendix A, Eq. (A.14), where σ_{in}^{NN} is the total inelastic NN cross section. Then, according to derivation, Eq. (A.14) describes the total inelastic cross section on a nucleus minus the part related to quasielastic nuclear excitations (with no hadron produced). This is not what was actually measured in any of the three experiments [1–3]. These experiments have different event selections and the calculations should comply with that.

The STAR experiment triggers on forward neutrons from the gold [2] and detects all inelastic $d-Au$ collisions including quasielastic excitation of the gold[1]. In this case, according to the Glauber formalism presented in Appendix A, one should rely on Eq. (A.10) with $\sigma_{tot}^{NN} = 51\,\text{mb}$, rather than $\sigma_{in}^{NN} = 42\,\text{mb}$. At the same time, the two other spectrometers, PHENIX and PHOBOS, seem to be insensitive to large rapidity gap events, i.e. diffractive excitations of the deuteron and gold [1, 3][2]. Then Eq. (A.14) should be applied with a replacement $\sigma_{in}^{NN} \Rightarrow \sigma_{in}^{NN} - 2\sigma_{sd}^{NN} - \sigma_{dd}^{NN} \approx 30\,\text{mb}$, i.e. the single and double diffraction must be subtracted (see details in Sect. 2) [12, 13]. Apparently, it makes difference whether one performs calculations with input cross section 51 mb, or 42 mb, or 30 mb.

The numerator in (4), σ_{in}^{NN} is even more sensitive than the denominator to assumptions which inelastic channels should be included. However this does not seem to be a problem, since the cross section of high-p_T production in pp collisions, $d\sigma^{pp}/d^2p_T$, was directly measured in the all three experiments [3], and we consider only the nuclear modification factor Eq. (5) in what follows.

1.3 The outline

This paper is organized as follows. We present a brief and simple derivation of basic formulae of the Glauber model [16] in Appendix A. In Sect. 2 we treat the deuteron as a nucleus and generalize the Glauber model for this case. We derive formulae for the cross sections of different channels, perform numerical calculations and present the results in Table 1. We corrected the input inelastic NN cross section for diffraction and found a smaller σ_{in}^{dA} than in [1, 3], but larger than in [2].

Events with a tagged spectator nucleon may serve as a sensitive probe for nuclear transparency, since the spectator must propagate through the nucleus with no interaction. We calculate the total cross section for this channel and the transverse momentum distribution of the spectators. On the contrary to naive expectation that noninteracting nucleons retain their primordial Fermi momentum distribution, we found an amazingly strong focusing effect. Namely, the nucleus acts like a lens focusing the spectators into a narrow cone

[1] I appreciate the very informative communication with Carl Gagliardi on this issue.

[2] A part of diffraction might have been included into the trigger efficiency of the PHENIX spectrometer. Namely, double diffraction, i.e. excitation of nucleons in both the deuteron and gold can reach and fire sometimes the closest of the two BBC triggers covering pseudorapidity intervals $\eta = \pm(3 - 3.9)$. However, the main part of diffraction, single diffractive excitation of either the deuteron, or gold, hardly could reach the opposite hemisphere and fire both the BBC triggers simultaneously, what is the trigger condition. I am thankful to Barbara Jacak and Sasha Milov for informative and clarifying discussions of this issue.

[3] Although it is stated in [1] that the cross section $d\sigma^{pp}/d^2p_T$ was normalized to 42 mb, in fact it was measured [14, 15].

with momentum transfer range of the order of the inverse nuclear radius. The transverse momentum spectrum of the spectators acquires typical diffraction structure having minima and maxima.

Inelastic shadowing corrections are introduced in Sect. 4. First, we use the traditional presentation in terms of inelastic diffractive excitations in intermediate state of hadron-nucleus elastic amplitude (Sect. 4.1). This approach is quite restricted, being unable to deal with higher order scattering terms which are especially important at high energies. Therefore, we switch to the eigenstate representation introduced in general terms in Sect. 4.2. Its realization in QCD is the light-cone color-dipole approach presented in Sect. 5.

The part of the inelastic corrections related to the lowest hadronic Fock component consisted only of valence quarks corresponds to diffractive excitation of resonances in usual terms. This contribution is analyzed and estimated numerically in Sect. 5.1. We demonstrate that this corrections make heavy nuclei much more transparent: instead of exponential attenuation we found a linear dependence on the inverse nuclear thickness (Sect. 5.1.1). Correspondingly, we derived formulae for cross sections of different channels corrected for inelastic shadowing for hadron-nucleus (Sect. 5.1.2), and deuteron-nucleus (Sect. dA) collisions. In Sect. 5.3 we study possibility to improve our calculations. We tested sensitivity of our results to the form of the nucleon wave function, and derived formulae for the case of a realistic saturated dipole-nucleon cross section.

Gluonic excitations corresponding to Fock states containing extra gluons are considered in Sect. 6. They correspond to diffractive excitations of large mass which are known to have quite a small cross section. This smallness leads to a prediction of rather weak gluonic shadowing, $\sim 20\%$, and small contribution to the inelastic corrections. At the same time other models predict much stronger gluon shadowing (Sect. 6.2) which may substantially change the normalization of the dAu data.

Since nuclear matter become more transparent due to inelastic shadowing, the number of participants changes as well. In Sect. 6.3 we found this effect to be sizeable.

In Sect. 7 we sum up the effects considered so far to see how much they affect the dAu data. The results are presented in Table 1. We also corrected the PHENIX data for high-p_T pions to see how important are these corrections compared to the current error bars. We found a considerable change: the Cronin effect for high-p_T pions disappeared.

Our observations are summarized in Sect. 8. The main conclusion is that the current data for high-p_T hadron production in deuteron-gold collisions are not decisive, and should be complemented with direct measurements of the inelastic dAu cross section.

2 Extending the Glauber model to deuteron-nucleus collisions

The basic formulae of Glauber model for hadron-nucleus collisions are presented in Appendix A. If to treat the deuteron as a hadron, one can calculate the dA total, total elastic and inelastic cross section provided that the elastic dN amplitude is known. The latter can be calculated employing the Glauber model too. This is done in Appendix A.

One can do calculations differently, treating the deuteron as a system of two nucleons interacting with the nucleus. In this case one can consider more reaction channels as deuteron excitation etc., which are missed in the previous approach.

2.1 The total cross section

. We generalize Eq. (A.5) from Appendix A for a deuteron beam as following,

$$\begin{aligned}\sigma_{tot}^{dA} &= 2\mathrm{Re}\int d^2r_T\ |\Psi_d(r_T)|^2 \\ &\times \left\langle 0\left|1-\prod_{k=1}^{A}\left[1-\Gamma^{pN}(\vec{b}-\vec{r}_T/2-\vec{s}_k)\right]\left[1-\Gamma^{nN}(\vec{b}+\vec{r}_T/2-\vec{s}_k)\right]\right|0\right\rangle \\ &= 2\int d^2b\int d^2r_T\ |\Psi_d(r_T)|^2\left\{1-\exp\left[-\frac{1}{2}\,\sigma_{tot}^{NN}\,\left(T_A^N(\vec{b}+\frac{1}{2}\vec{r}_T)+T_A^N(\vec{b}-\frac{1}{2}\vec{r}_T)\right)\right.\right. \\ &+ \left.\left.\sigma_{el}^{NN}\,T_A^N(b)\,\exp\left(-\frac{r_T^2}{4B_{NN}}\right)\right]\right\} \qquad (7)\end{aligned}$$

where $\vec{r}_T$ is the transverse nucleon separation in the deuteron; $|\Psi_d(r_T)|^2$ is the deuteron light-cone wave function squared and integrated over relative sharing by the nucleons of the deuteron longitudinal momentum. It is presented in Appendix B. The effective nuclear thickness function, $T_A^N(b)$, convoluted with the NN elastic amplitude is introduced in (A.6).

We did calculations with nuclear density in the Woods-Saxon form

$$\rho_A(r)=\frac{3\,A}{4\pi R_A^3(1+\pi^2a^2/R_A^2)}\,\frac{1}{1+\exp\left(\frac{r-R_A}{a}\right)} \qquad (8)$$

with $R_A = 6.38\,\mathrm{fm}$ and $a = 0.54\,\mathrm{fm}$, same as in [1] for easier comparison. The result for the total cross section σ_{tot}^{dAu} is shown in Table 1.

Eq. (7) is easy to interpret. The two first term in the exponent correspond to independent interaction of two nucleons separated by transverse distance $\vec{r}_T$. Of course, the smaller r_T is, the stronger nucleons shadow each other, and this is accounted for by the third term.

One can see the difference between this expression and Eq. (A.5) (for $h \equiv d$). In the latter cases the averaging over $\vec{r}_T$ is put up into the exponent, while in the former case, Eq. (7), the whole exponential is averaged. We will see in Sect. 4.2 that this difference is a part of the Gribov's inelastic corrections, so (7) makes the first step beyond the Glauber approximation.

Note that the last term in the exponent in (7) is quite small. Besides smallness of $\sigma_{el}^{NN}/\sigma_{tot}^{NN}$, the exponential factor is rather small. The mean value of the exponent is $\langle r_T^2\rangle/4B_{NN} \approx 5$. This term reduces the total $d-Au$ cross section by 1.3% only.

2.2 The cross section of elastic dA scattering and deuteron breakup $dA \to pnA$

.

Table 1: *Results for different cross sections and numbers of collisions calculated using Glauber approximation (Sect. 2), corrected for inelastic shadowing related to valence quark fluctuations (Sect. 5.1), and for gluon shadowing (Sect. 6). The results including the ultimate renormalization factor K depend on the experimental set up and are different for the STAR and PHENIX experiments*

	Observable	Glauber model	Valence quark fluctuations	Plus gluonic excitations	Correction factor
	σ_{tot}^{dAu}[mb]	4110.1	3701.0	3466.2	
S	σ_{in}^{dAu}[mb]	2422.7	2226.6(2335.8)	2118.3(2228.3)	
T	Factor K in (5)-(6)	K_{GL} =1.04		$K_{Gr} = 0.87(0.92)$	K=0.91(0.96)
A	$N_{coll}^{in}(min.b.)$	6.9	7.5	7.9	
R	$\sigma_{in}^{dAu}(tagg)$[mb]	458.4	544.9(511.5)	551.8(520.1)	
	$N_{coll}^{in}(tagg)$	2.9	4.4	5.0	
P	$\sigma_{non-diff}^{dAu}$[mb]	2146.0	1998.3(2100.1)	1930.3(2033.7)	
H	Factor K	$K_{Gl} = 0.92$		$K_{Gr} = 0.9(0.95)$	K=0.83(0.87)
E	$N_{coll}^{non-diff}(min.b.)$	5.5	5.9	6.1	
N	$\sigma_{non-diff}^{dAu}(tagg)$[mb]	324.3	480.2(451.5)	498.4(470.6)	
I	$N_{coll}^{non-diff}(tagg)$	2.3	2.9	3.2	
X					

According to (A.9) in order to find elastic dA cross section one should square the partial elastic amplitude and integrate over b,

$$\sigma_{el}^{dA} = \int d^2b \left| \int d^2r_T \ |\Psi_d(r_T)|^2 \left\{ 1 - \exp\left[-\frac{1}{2}\sigma_{tot}^{NN} \left(T_A^N(\vec{b} + \frac{1}{2}\vec{r}_T) + T_A^N(\vec{b} - \frac{1}{2}\vec{r}_T) \right) \right. \right. \right.$$
$$\left. \left. \left. + \ \sigma_{el}^{NN} \, T_A^N(b) \, \exp\left(-\frac{r_T^2}{4B_{NN}} \right) \right] \right\} \right|^2 \qquad (9)$$

This is the square of the average of the elastic amplitude over deuteron configurations.

If, however, to take average of the amplitude squared, that will include also dissociation $d \to pn$, i.e.

$$\begin{aligned}\sigma_{el}^{dA}(dA \to dA) + \sigma_{diss}^{dA}(dA \to npA) &= \int d^2b \int d^2r_T \; |\Psi_d(r_T)|^2 \\ &\times \left| 1 - \exp\left[-\frac{1}{2}\sigma_{tot}^{NN} \left(T_A^N(\vec{b} + \frac{1}{2}\vec{r}_T) + T_A^N(\vec{b} - \frac{1}{2}\vec{r}_T) \right) \right.\right. \\ &+ \left.\left. \sigma_{el}^{NN}\, T_A^N(b)\, \exp\left(-\frac{r_T^2}{4B_{NN}} \right) \right] \right|^2 \qquad (10)\end{aligned}$$

2.3 The total inelastic cross section

Subtracting from the total cross section the elastic part one gets the cross section of all inelastic channels in $d - A$. We, however, prefer to subtract the deuteron quasielastic breakup too, since it is not detected by any of the RHIC experiments. Then we have,

$$\begin{aligned}\sigma_{in}^{dA} &= \sigma_{tot}^{dA} - \sigma_{el}^{dA} - \sigma_{diss}^{dA}(dA \to npA) = \int d^2b \int d^2r_T \; |\Psi_d(r_T)|^2 \\ &\times \left\{ 1 - \exp\left[-\sigma_{tot}^{NN} \left(T_A^N(\vec{b} + \frac{1}{2}\vec{r}_T) + T_A^N(\vec{b} - \frac{1}{2}\vec{r}_T) \right) \right.\right. \\ &+ \left.\left. 2\,\sigma_{el}^{NN}\, T_A^N(b)\, \exp\left(-\frac{r_T^2}{4B_{NN}} \right) \right] \right\} \; . \qquad (11)\end{aligned}$$

The result of numerical calculation for this cross section is exposed in Table 1. This cross section covers diffractive excitations as well, therefore we place the result in the upper panel of the table which is supposed to be related to experiments sensitive to diffraction (STAR).

The impact parameter distribution of the inelastic cross section is plotted by dashed curve in Fig. 2, and the integrated cross section is shown in Table 1.

2.4 The cross section of nondiffractive channels

.

In experiments insensitive to large rapidity gap event one should employ the inelastic cross section with all diffractive contribution is removed. Namely, one should also subtract the cross sections of quasielastic excitation of the nucleus, $A \to A^*$, and diffractive excitation of colliding nucleons.

The cross section of single ($dA \to dA^*$) and double ($dA \to pdA^*$) quasielastic and quasidiffractive nuclear excitation reads [compare with (A.13)],

$$\begin{aligned}&\sigma_{qel}^{dA}(dA \to dA^*) + \sigma_{qsd}^{dA}(dA \to pnA^*) = \int d^2r_T \; |\Psi_d(r_T)|^2 \\ &\times \left\{ \left\langle 0 \left| \left| 1 - \prod_{k=1}^{A} \left[1 - \Gamma^{pN}(\vec{b} - \vec{r}_T/2 - \vec{s}_k) \right] \left[1 - \Gamma^{nN}(\vec{b} + \vec{r}_T/2 - \vec{s}_k) \right] \right|^2 \right| 0 \right\rangle \right. \\ &- \left. \left\langle 0 \left| 1 - \prod_{k=1}^{A} \left[1 - \Gamma^{pN}(\vec{b} - \vec{r}_T/2 - \vec{s}_k) \right] \left[1 - \Gamma^{nN}(\vec{b} + \vec{r}_T/2 - \vec{s}_k) \right] \right| 0 \right\rangle^2 \right\}\end{aligned}$$

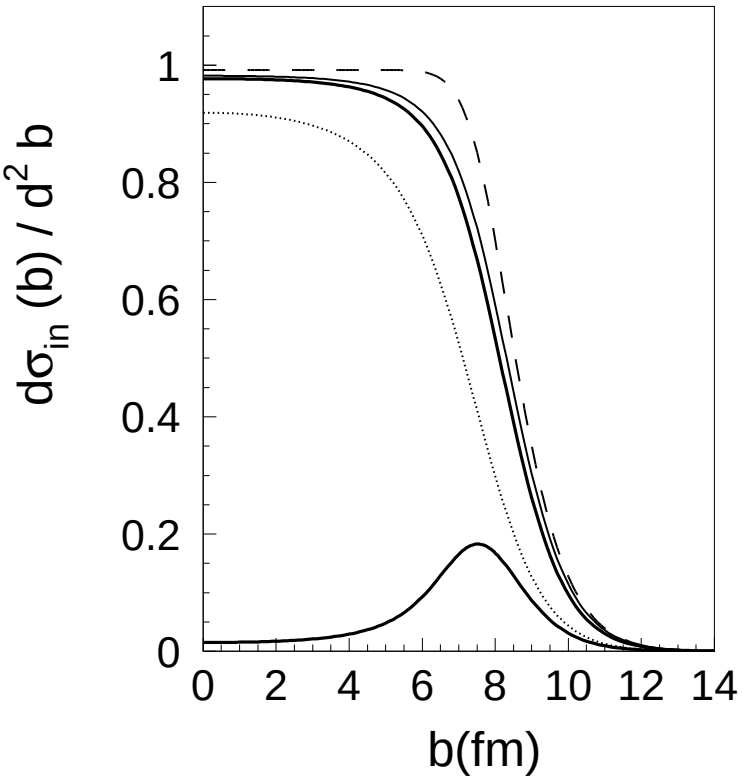

Figure 2: *The impact parameter distribution of inelastic deuteron-gold collisions (three upper curves) including diffractive excitations (STAR trigger). Impact parameter $\vec{b}$ corresponds to center of gravity of the deuteron. The dashed curve corresponds to the Glauber approximation Eq. (10). The thin solid curve include inelastic shadowing related to excitation of the valence quark skeleton, Eq. (45). The thick solid curve is final, it includes gluon shadowing as well. The bottom solid thick curve shows the difference between the Glauber and final curves. The dotted curve shows the range of model uncertainty and corresponds to gluon shadowing with $R_G = 03$ (see Sect. 6.2). All curves are calculated with total cross section $\tilde{\sigma}_{tot}^{NN} = 51\, mb$.*

$$
\begin{aligned}
= & \int d^2b \int d^2r_T \; |\Psi_d(r_T)|^2 \left\{ \exp\left[-\sigma_{in}^{NN} \left(T_A^N(\vec{b}+\frac{1}{2}\vec{r}_T) + T_A^N(\vec{b}-\frac{1}{2}\vec{r}_T) \right) \right. \right. \\
+ & \left. 4\,\sigma_{el}^{NN}\, T^N(b)\, \gamma(r_T)\, \exp\left(-\frac{r_T^2}{4B_{NN}} \right) \right] \\
- & \left. \exp\left[-\sigma_{tot}^{NN} \left(T_A^N(\vec{b}+\frac{1}{2}\vec{r}_T) + T_A^N(\vec{b}-\frac{1}{2}\vec{r}_T) \right) + \sigma_{el}^{NN} T^N(b) \exp\left(-\frac{r_T^2}{4B_{NN}} \right) \right] \right\}, \quad (12)
\end{aligned}
$$

where

$$
\gamma(r) = 1 - \frac{8}{3}\,\frac{\sigma_{el}^{NN}}{\sigma_{tot}^{NN}}\, \exp\left(-\frac{r_T^2}{8B_{NN}} \right) + 8 \left(\frac{\sigma_{el}^{NN}}{\sigma_{tot}^{NN}} \right)^2 \exp\left(-\frac{r_T^2}{4B_{NN}} \right) \; , \qquad (13)
$$

is a correction factor hardly different from one. In what follows we do not keep the small terms in (13). Note that the form of Eq. (12) is analogous to that of Eq. (A.13).

For experiments insensitive to diffraction the quasielastic cross section Eq. (12) should be subtracted (11) and the result will be similar to Eq. (A.14). However, we still miss the contribution of diffractive channels related to diffractive excitations of nucleons in the deuteron and nucleus. It is impossible to introduce consistently diffraction in the framework of the Glauber model which is a single channel approximation. Diffraction naturally emerges in the multiple coupled channel approach or in the eigenstate method introduced below. Meanwhile, one can use the following prescription.

Let us expand the exponentials in (12) in small expansion parameter $\sigma_{el}^{NN}\,T_A(b)$ up to the first order,

$$\begin{aligned}\sigma_{qel}^{dA} &\approx \int d^2b \int d^2r_T\ |\Psi_d(r_T)|^2\ \exp\left[-\sigma_{tot}^{NN}\ \left(T_A^N(\vec{b}+\frac{1}{2}\vec{r}_T)+T_A^N(\vec{b}-\frac{1}{2}\vec{r}_T)\right)\right] \\ &\times\ \sigma_{el}^{NN}\ \left[T_A^N(\vec{b}+\frac{1}{2}\vec{r}_T)+T_A^N(\vec{b}-\frac{1}{2}\vec{r}_T)\right]+... \end{aligned} \tag{14}$$

In order to include the possibility of diffractive excitation of nucleons in the colliding nuclei, one should replace in (14)

$$\sigma_{el}^{NN} \Rightarrow \tilde{\sigma}_{el}^{NN} = \sigma_{el}^{NN} + 2\sigma_{sd}^{NN} + \sigma_{dd}^{NN}\ . \tag{15}$$

in all orders of $\sigma_{el}^{NN}\,T_A(b)$. This is a substantial correction since at RHIC energy $\sigma_{el}^{NN} = 9\,\mathrm{mb}$, and $\sigma_{el}^{NN} + 2\sigma_{sd}^{NN} + \sigma_{dd}^{NN} = 21\,\mathrm{mb}$.

The final Glauber model expression for the non-diffractive inelastic dA cross section reads,

$$\begin{aligned}\sigma_{non-diff}^{dA} &= \int d^2b \int d^2r_T\ |\Psi_d(r_T)|^2 \left\{1-\exp\left[-\tilde{\sigma}_{in}^{NN}\ \left(T_A^N(\vec{b}+\frac{1}{2}\vec{r}_T)+T_A^N(\vec{b}-\frac{1}{2}\vec{r}_T)\right)\right.\right. \\ &+ \left.\left. 4\,\tilde{\sigma}_{el}^{NN}\,T_A^{NN}(b)\ \exp\left(-\frac{r_T^2}{4B_{NN}}\right)\right]\right\} \end{aligned} \tag{16}$$

where

$$\tilde{\sigma}_{in}^{NN} = \sigma_{tot}^{NN} - \tilde{\sigma}_{el}^{NN} \tag{17}$$

We calculated the non-diffractive part, Eq. (16), of the inelastic $d-Au$ cross section, and the result is shown in Table 1. The corresponding number of collisions also presented in the Table is rather small compared to the one quoted in [1]. This is mainly due to a smaller inelastic cross section $\tilde{\sigma}_{in}^{NN}$ we use.

3 Quantum mechanics at work: illuminating focusing effect for spectators

Assume that only the proton in the deuteron interacts inelastically with the nucleus, while the neutron is a spectator (of course all following results are symmetric relative to interchange $p \leftrightarrow n$). This is a very interesting process of simultaneous interaction and no interaction. It provides direct information about nuclear transparency. Apparently, this process

pushes the neutron to the ultra-periphery of the nucleus where its survival probability is high, while the proton prefers to hit the dense area of the nucleus and interact.

Naively, the survived spectator neutrons should maintain their primordial transverse momentum distribution controlled by the deuteron size. This is assumed in the Glauber Monte Carlo. However, quantum mechanics is at work, and the nucleus acts like a lens focusing spectator neutrons. The survival probability modifies the shape of the wave packet of the spectators in the impact parameter plane. Correspondingly, their p_T-distribution changes. This is how elastic scattering on an absorptive target happens: it is not due to transparency of the target, but is caused by absorption. In the limit of a completely transparent target, the incoming plane wave is not disturbed and no scattering occurs. Absorption makes a hole in the plane wave, and one can think about the outside area of the incoming wave which undergoes elastic scattering. On the other hand, one can subtract the incoming plane wave whose Fourier transform is just a delta function (zero angle scattering) and the rest is a wave packet with a transverse area of the target size. A Fourier transform of this wave packet gives the elastic amplitude [compare with (A.9)].

Thus, the spectator neutrons experience elastic scattering on the target, rather than simply propagate with the undisturbed primordial transverse Fermi momentum. Below we derive formulas which show how elastic scattering of the spectator neutrons happens, and perform numerical evaluation of the effect.

We start with the cross section of this process which can be written as,

$$\begin{aligned}\sigma^{dA}_{tagg}(dA\to nX) &= \mathrm{Re}\int d^2r_T\ |\Psi_d(r_T)|^2 \left\langle 0\left|\prod_{k=1}^{A}\left[1-\Gamma^{nN}\left(\vec{b}-\vec{r}_T-\vec{s}_k\right)\right]^2\right.\right. \\ &\times \left.\left\{1-\prod_{k=1}^{A}\left[1-2\,\Gamma^{pN}\left(\vec{b}-\vec{s}_k\right)\right]\right\}\right|0\right\rangle\ , \end{aligned} \tag{18}$$

where $\vec{b}$ is the impact parameter of the proton. The first factor here would be the elastic neutron-nucleus cross section, if it were not weighted by the second term which is the inelastic proton-nucleus cross section, i.e. the difference between the total and elastic and quasielastic cross sections (see Appendix A).

After integration over the coordinates of bound nucleons we get,

$$\begin{aligned}&\sigma^{tagg}_{non-diff}(dA\to nX) = \int d^2b\int d^2r_T\ |\Psi_d(r_T)|^2\ \exp\left[-\sigma^{NN}_{tot}\,T^N_A\left(\vec{b}-\vec{r}_T\right)\right] \\ &\times\ \left\{1-\exp\left[-\tilde{\sigma}^{NN}_{in}\,T^N_A\,(b)+4\,\sigma^{NN}_{el}\,T^N(\vec{b}-\vec{r}_T/2)\,\gamma(r_T)\,\exp\left(-\frac{r_T^2}{4B_{NN}}\right)\right]\right\}\end{aligned} \tag{19}$$

Here we made a correction for diffractive channels replacing $\sigma^{NN}_{in}\Rightarrow\tilde{\sigma}^{NN}_{in}$ and $\sigma^{NN}_{el}\Rightarrow\tilde{\sigma}^{NN}_{el}$, valid only for those experiment which are not sensitive to diffraction (PHENIX, PHOBOS). Correspondingly, the numerical result for $\sigma^{tagg}_{non-diff}(dA\to nX)$ is placed at the bottom part of the Table. The results at the upper part of the Table use the total elastic and total cross sections instead of $\tilde{\sigma}^{NN}_{el}$ and $\tilde{\sigma}^{NN}_{in}$ as an input for calculations. Indeed, since the STAR experiment is sensitive to quasielastic nuclear excitation as well, it should be included, and one has to rely on Eq. (A.13). We also demonstrate the impact parameter

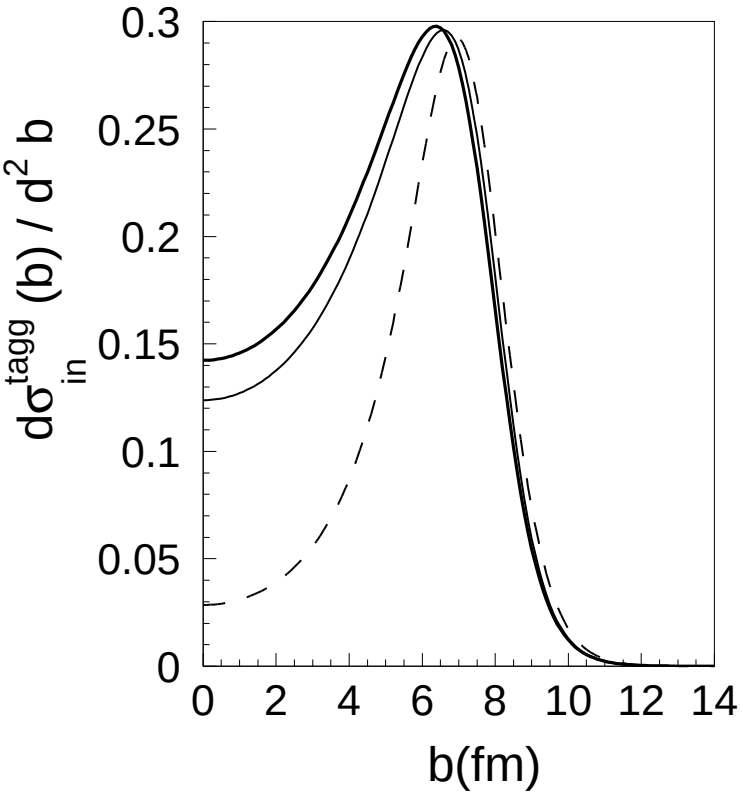

Figure 3: *The impact parameter distribution of interacting protons in tagged deuteron-gold collisions with spectator neutrons. The calculation includes diffractive excitations (STAR trigger). Impact parameter* $\vec{b}$ *corresponds to the proton. The dashed curve represents the Glauber approximation Eq. (10). The thin solid curve include inelastic shadowing related to excitation of the valence quark skeleton, Eq. (45). The thick solid curve includes gluon shadowing as well. All curves are calculated with total cross section* $\tilde{\sigma}_{tot}^{NN} = 51\, mb$.

dependence of $\sigma_{in}^{tagg}(dA \to nX)$ in Fig. 3. Interesting that the interacting protons in tagged dA collisions strongly pick at the very edge of the nucleus in spite of the large radius of the deuteron. This is not a trivial observation which can be probably interpreted as follows. The spectator neutron must be mostly outside of the nucleus. Then, for a protons which are close to the edge of the nucleus the interval of azimuthal angle between the proton and neutron is larger than for a proton deep inside the nuclear area. This phase space factor enhances the contribution of peripheral protons.

To see how the spectator neutrons are distributed one can use the same Eq. (19) with the replacement $\vec{b} \Rightarrow \vec{b} + \vec{r}_T$. The result of calculations is depicted in Fig. 4. This plot demonstrates that the spectators have a more peripheral impact parameter distribution than the interacting protons, but they are amazingly close.

We also calculated the number of collisions of the proton which underwent interaction

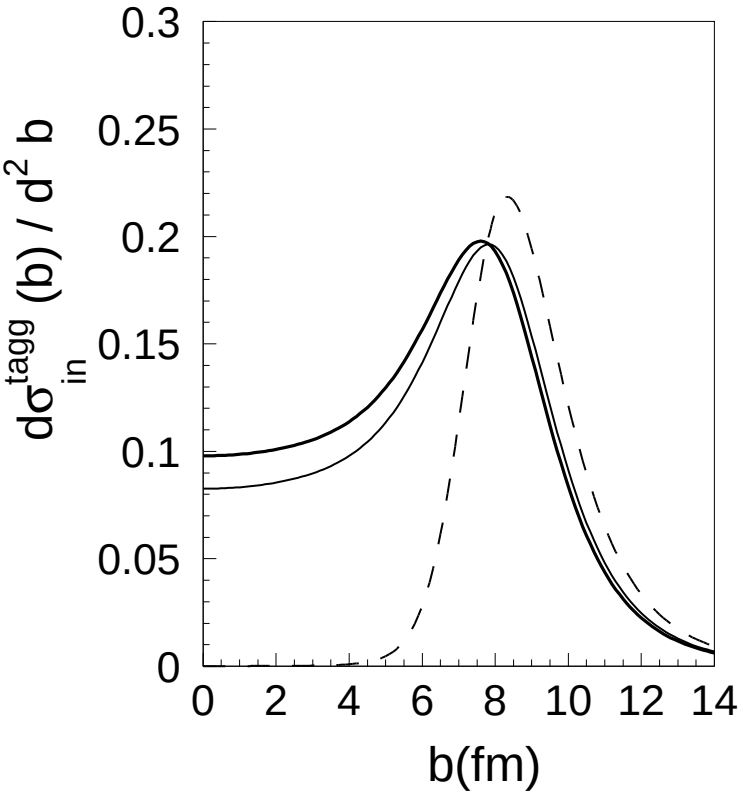

Figure 4: *The impact parameter distribution of spectator neutrons in tagged deuteron-gold collisions with interacting protons. The calculation includes diffractive excitations (STAR trigger). Impact parameter* $\vec{b}$ *corresponds to the proton. The dashed curve represents the Glauber approximation Eq. (10). The thin solid curve include inelastic shadowing related to excitation of the valence quark skeleton, Eq. (45). The thick solid curve includes gluon shadowing as well. All curves are calculated with total cross section* $\tilde{\sigma}_{tot}^{NN} = 51\, mb$.

in events with a tagged spectator neutron,

$$N_{coll}^{tagg} = \frac{\tilde{\sigma}_{in}^{NN}}{\sigma_{tagg}^{dA}} \int d^2b \int d^2r_T \; |\Psi_d(r_T)|^2 \; T_A^N(\vec{b} + \vec{r}_T/2) \; \exp\left[-\sigma_{tot}^{NN} \, T_A^N(\vec{b} - \vec{r}_T/2)\right] \qquad (20)$$

The results for N_{coll}^{tagg} for events which include diffraction or do not are shown at the upper and bottom panels of Table 1 respectively. The mean value of N_{coll} for tagged events turns out to be nearly a half of the minimal bias value, Eq. (3), which is for two nucleons in the deuteron. This contradicts the intuitive expectation that tagged events are much more peripheral than minimum bias inelastic collisions and the proton should have a much smaller number of collisions.

To get the transverse momentum distribution of spectator neutrons, one should Fourier

transform the elastic neutron amplitude before squaring it,

$$\begin{aligned}\frac{d\sigma_{tagg}(dA\to nX)}{d^2q_T} &= \frac{1}{(2\pi)^2}\int d^2b\left\{1-\exp\left[-\tilde{\sigma}_{in}^{NN}\,T_A^N(b)\right]\right\}\int d^2r_1\,d^2r_2\\ &\times \exp\left[i\vec{q}_T(\vec{r}_1-\vec{r}_2)\right]\exp\left\{-\frac{1}{2}\,\sigma_{tot}^{NN}\,\left[T_A^N\left(\vec{b}-\vec{r}_1\right)+T_A^N\left(\vec{b}-\vec{r}_2\right)\right]\right\}\\ &\times \int\limits_{-\infty}^{\infty}dr_L\left[\frac{u^*(r_L,r_1)u(r_L,r_2)+w^*(r_L,r_1)w(r_L,r_2)}{\sqrt{(r_L^2+r_1^2)(r_L^2+r_2^2)}}\right],\end{aligned}\tag{21}$$

Important is that the proton inelastic interaction is incoherent, therefore we should first sum up coherently all amplitudes of neutron elastic scattering for the fixed impact parameter of the proton, then Fourier transform it, square and after all integrate over the proton impact parameter. This is explicitly done in (21). Apparently, integration over $\vec{q}_T$ in (21) leads to the expression in Eq. (19). The S and D wave functions are presented in Appendix B.

In Fig. 5 we compare the normalized differential cross section Eq. (21),

$$R_{tagg}(q_T)=\frac{1}{\sigma_{in}^{tagg}}\,\frac{d\sigma_{tagg}^{dA}}{d^2q_T}\tag{22}$$

with the undisturbed primordial distribution of the neutron in the incoming deuteron, also normalized to one,

$$\begin{aligned}\frac{dN_n^d}{d^2q} &= \frac{1}{(2\pi)^2}\int d^2r_1\,d^2r_2\exp\left[i\vec{q}_T(\vec{r}_1-\vec{r}_2)\right]\\ &\times \int\limits_{-\infty}^{\infty}dr_L\left[\frac{u^*(r_L,r_1)u(r_L,r_2)+w^*(r_L,r_1)w(r_L,r_2)}{\sqrt{(r_L^2+r_1^2)(r_L^2+r_2^2)}}\right],\end{aligned}\tag{23}$$

The surprising observation is that the spectator neutrons have a much narrower q_T-distribution than the Fermi motion in the deuteron. This is opposite to the usual q_T-broadening (Cronin effect) for particles propagating though a matter [61]. In the present case the nucleus acts like a lens focusing neutrons. Fig. 5 also exposes quite a different shape of the q_T-distribution of spectators having diffraction-like minima and maxima.

If to compare the mean values of q_T^2 of spectator neutrons with the primordial value in the deuteron, the difference is tremendous, about factor 20.

$$\langle q_T^2\rangle_{spect} = 0.00038\,\mathrm{GeV}^2\tag{24}$$

$$\langle q_T^2\rangle_{deuteron} = 0.0065\,\mathrm{GeV}^2\tag{25}$$

This focusing effect is a beautiful manifestation of quantum mechanics. The intuitive interpretation is rather straightforward. The condition that the neutron in the deuteron remains intact, while the proton must interact, means that the neutron tries to pass the nucleus through the diluted periphery, while the proton prefers the collision to be central. These conflicting conditions cause a strong suppression of small-size deuteron fluctuations,

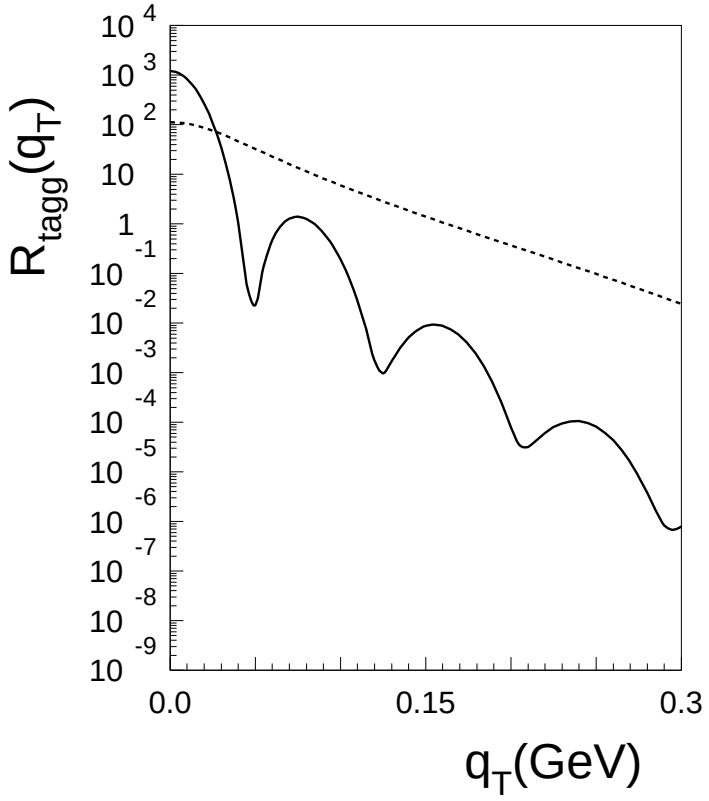

Figure 5: *Transverse momentum distribution of spectator neutrons in the tagged reaction $d + Au \to n + X$ (solid curve), and in the projectile deuteron (dashed curve). The inelastic reaction $p + Au \to X$ is assumed to include diffraction (STAR experiment). The calculations are performed in the Glauber approximation, Eq. (21).*

while large separations in the deuteron are enhanced. Apparently, such large size configurations are related to a smaller Fermi momentum and this simple observation explains the focusing effect.

This explanation offers a possibility to study the correlation of the focusing effect with centrality of collision[4]. Suppressing b-integration in (21) one can trace the b-dependence of the focusing effect. In Fig. 6 the same comparison of two q_T-distributions is shown for central collision $b = 0$ (impact parameter of the interacting proton). The interpretation of central collisions is especially clear. Once the proton hits the center of the nucleus, the spectator neutron must be located along a rage ring outside of the nucleus with a radius larger than the nucleus. Correspondingly, the q_T-distribution has the typical diffractive shape and a small width $\Delta q_T \lesssim 1/R_A$.

On the contrary to our expectations, the distributions are quite similar. The mean value of $\langle q_T^2 \rangle = 0.00032\,\mathrm{GeV}^2$ is close to our result Eq. (24) for the minimal bias sample.

One may wonder why the minima on the q_T-distribution Fig. 6 are deeper than for min-

[4]I am thankful to Alexei Denisov for this suggestion.

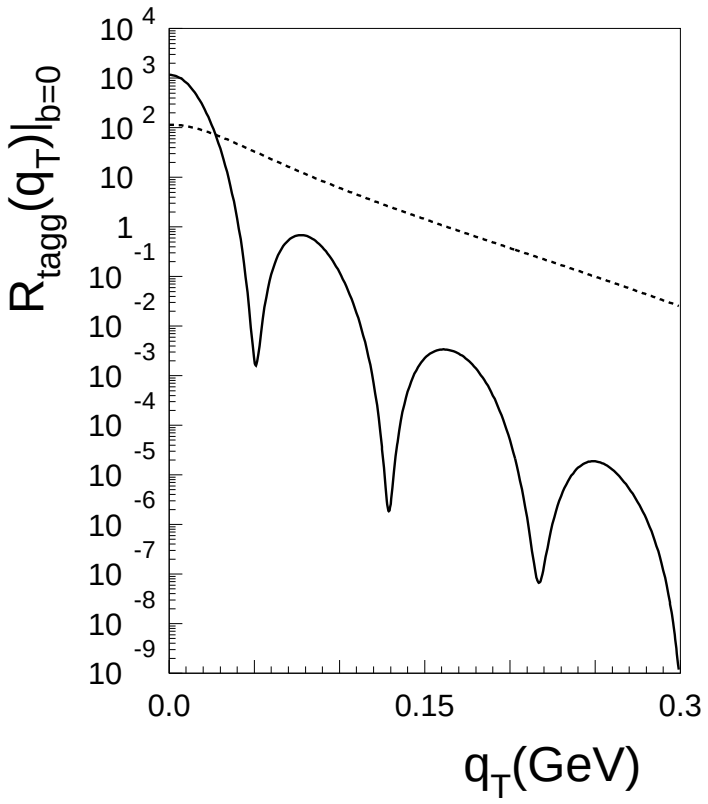

Figure 6: *Same as in Fig. 5, but for a central ($b = 0$) proton-gold collision, accompanied by a spectator neutron.*

imal bias sample Fig. 5. In fact, for central collisions the minima go down to zero, since we neglected the real part of the elastic amplitude and the Fourier transform oscillates changing sign. However, the position of the minima (slightly) depend on the impact parameter of the collision. Therefore, when one sums up q_T-distributions with different minimum positions, the resulting distribution will have minima which are partially filled up.

One should be cautious comparing these predictions with data which might be contaminated by non-spectator neutrons. First, the neutron calorimeters used at RHIC have a rather large acceptance which covers transverse momenta up to $\sim 300\,\mathrm{MeV}$. Therefore, most of the neutrons which experienced quasielastic scattering contribute as well (except STAR). Besides, the range of longitudinal momenta is rather large and events with diffractive excitation on nucleons in the gold should contribute too. All such neutrons are not spectators and have much wider q_T-distribution.

Second, selecting central collisions in accordance with higher multiplicity, one should remember that central collisions are suppressed (see Fig. 3) and one should not mix them up with the fluctuations of multiplicity.

4 Inelastic shadowing corrections

4.1 Intermediate state diffractive excitations

The Glauber model is a single-channel approximation, it misses the possibility of diffractive excitation of the projectile in intermediate state illustrated in Fig. 7. These corrections

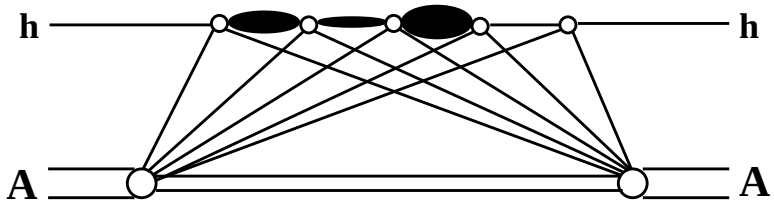

Figure 7: *Diagonal and off-diagonal diffractive multiple interactions of the projectile hadron in intermediate state.*

called inelastic shadowing were introduced by Gribov back in 1969 [9]. The formula for the inelastic corrections to the total hadron-nucleus cross section was suggested in [17],

$$\begin{aligned}\Delta\sigma_{tot}^{hA} &= -4\pi\int d^2b\exp\left[-\frac{1}{2}\,\sigma_{tot}^{hN}\,T_A(b)\right]\int\limits_{M^2_{min}} dM^2\;\left.\frac{d\sigma_{sd}^{hN}}{dM^2\,dp_T^2}\right|_{p_T=0}\\ &\times\int\limits_{-\infty}^{\infty} dz_1\,\rho_A(b,z_1)\int\limits_{z_1}^{\infty} dz_2\,\rho_A(b,z_1)\,e^{iq_L(z_2-z_1)}\;,\end{aligned}\tag{26}$$

where σ_{sd}^{hN} is the cross section of single diffractive dissociation $hN\to XN$ with longitudinal momentum transfer

$$q_L=\frac{M^2-m_h^2}{2E_h}\;.\tag{27}$$

This correction makes nuclei more transparent [18]. One can also see from Fig. 1 that (26) does a good job describing data at low energies [10,19], since takes care of the onset of inelastic shadowing via phase shifts controlled by q_L. Higher order off-diagonal transitions are neglected. Diagonal transitions (or absorption of the excited state) are important, but unknown. Indeed, the intermediate state X has definite mass M, but no definite size, or cross section. It is ad hoc fixed in (26) at σ_{tot}^{hN}. It has been a long standing problem how to deal simultaneously with phase shifts which are controlled by the mass, and with the cross section which depends on the size. This problem was eventually solved in [20,21] within the light-cone Green function approach (see Sect. 6).

The situation changes at the high energies of RHIC and LHC, all multiple interactions become important, but phase shifts vanish, substantially simplifying calculations. No experimental information, however, is available for off-diagonal diffractive amplitudes for excited state transitions $X_1\to X_2$. A solution proposed in [22] is presented in the next Sect. 4.2.

There is, however, one exclusion which is free of these problems, hadron-deuteron collisions. In this case no interaction in intermediate state is possible and knowledge of diffractive cross section $NN \to NX$ is sufficient to calculate the inelastic correction with no further assumptions. In this case Eq. (26) takes the simple form [9, 23], analogous to (A.17),

$$\Delta\sigma_{tot}^{hd} = -2 \int dM^2 \int dp_T^2 \, \frac{d\sigma_{sd}^{hN}}{dM^2 dp_T^2} \, F_d(t) \ . \tag{28}$$

We calculate this correction for pd collisions following [24] at $\sqrt{s} = 200\,\mathrm{GeV}$ using the slope $B_{NN}^{sd} = 10\,\mathrm{GeV}^{-2}$ reduced compared to $B_{NN}^{el} = 14\,\mathrm{GeV}^{-2}$ by $4\,\mathrm{GeV}^{-2}$ which is the proton vertex contribution to the elastic slope. The upper cut off imposed by the deuteron formfactor on integration over M^2 is quite high at this energy and we can use the free diffraction cross section $\sigma_{sd}^{NN} = 4\,\mathrm{mb}$ [12]. Then we find $\Delta\sigma_{tot}^{hd} = -1.75\,\mathrm{mb}$

4.2 Eigenstate method

If a hadron were an eigenstate of interaction, i.e. could undergo only elastic scattering (as a shadow of inelastic channels) and no diffractive excitation was possible, the Glauber formula would be exact and no inelastic shadowing corrections would be needed. This simple observation gives a hint that one should switch from the basis of physical hadronic states to a new one consisted of a complete set of mutually orthogonal states which are eigenstates of the scattering amplitude operator. This was the driving idea of description of diffraction in terms of elastic amplitudes [25, 26], and becomes a powerful tool for calculation of inelastic shadowing corrections in all orders of multiple interactions [22]. Hadronic states (including leptons, photons) can be decomposed into a complete set of such eigenstates $|k\rangle$,

$$|h\rangle = \sum_k \Psi_k^h \, |k\rangle \ , \tag{29}$$

where Ψ_k^h are hadronic wave functions in the form of Fock state decomposition. They obey the orthogonality conditions,

$$\begin{aligned} \sum_k \left(\Psi_k^{h'}\right)^\dagger \, \Psi_k^h &= \delta_{h\,h'} \ ; \\ \sum_h \left(\Psi_l^h\right)^\dagger \, \Psi_k^h &= \delta_{lk} \ . \end{aligned} \tag{30}$$

We denote by $f_{el}^{kN} = i\,\sigma_{tot}^{kN}/2$ the eigenvalues of the elastic amplitude operator $\hat{f}$ neglecting its real part. We assume that the amplitude is integrated over impact parameter, *i.e.* that the forward elastic amplitude is normalized as $|f_{el}^{kN}|^2 = 4\,\pi\,d\sigma_{el}^{kN}/dt|_{t=0}$. We can then express the elastic $f_{el}(hh)$ and off diagonal diffractive $f_{sd}(hh')$ amplitudes as,

$$f_{el}^{hN} = 2i \sum_k \left|\Psi_k^h\right|^2 \, \sigma_{tot}^{kN} \equiv 2i \, \langle\sigma\rangle \ ; \tag{31}$$

$$f_{sd}^{hN}(h \to h') = 2i \sum_k (\Psi_k^{h'})^\dagger \, \Psi_k^h \, \sigma_{tot}^{kN} \ . \tag{32}$$

Note that if all the eigen amplitudes were equal, the diffractive amplitude (32) would vanish due to the orthogonality relation, (30). The physical reason is obvious. If all the f_{el}^{kN} are equal, the interaction does not affect the coherence between the different eigen components $|k\rangle$ of the projectile hadron $|h\rangle$. Therefore, off diagonal transitions are possible only due to differences between the eigen amplitudes.

If one sums up all final states in the diffractive cross section one can use the completeness condition (30). Then, excluding the elastic channels one gets [22, 27, 28],

$$16\pi \left.\frac{d\sigma_{sd}^{hN}}{dt}\right|_{t=0} = \sum_i \left|\Psi_i^h\right|^2 \left(\sigma_{tot}^{iN}\right)^2 - \left(\sum_i \left|\Psi_i^h\right|^2 \sigma_{tot}^{iN}\right)^2 \equiv \langle\sigma_{tot}^2\rangle - \langle\sigma_{tot}\rangle^2 \ . \tag{33}$$

As far as the main problem of Glauber approximation is the need to include off-diagonal transitions, one should switch to an eigenstate basis. Then each of the eigen states can experience only elastic diffractive scatterings and the Glauber eikonal approximation becomes exact. Thus, all expressions for cross sections of different channels derived in Glauber approximation in Appendix A are exact for any of the eigenstates. Then, the corresponding cross sections for hadron-nucleus collisions are obtained via a proper averaging of those in Appendix A [22, 28],

$$\sigma_{tot}^{hA} = 2\int d^2b \left\{1 - \left\langle \exp\left[-\frac{1}{2}\,\sigma_{tot}\,T_A^h(b)\right]\right\rangle\right\} \tag{34}$$

$$\sigma_{el}^{hA} = \int d^2b \left|1 - \left\langle \exp\left[-\frac{1}{2}\,\sigma_{tot}\,T_A^h(b)\right]\right\rangle\right|^2 \tag{35}$$

$$\sigma_{in}^{hA} = \int d^2b \left\{1 - \left\langle \exp\left[-\sigma_{in}\,T_A^h(b)\right]\right\rangle\right\} \tag{36}$$

It is interesting that the last expression for σ_{in}^{hA} is already free of diffraction contribution. Although only elastic and quasi-elastic cross sections were subtracted from σ_{tot}^{hA} in Glauber model in Appendix A, after averaging over eigenstates it turns out that diffraction is subtracted as well. Indeed, direct averaging of the elastic cross section Eq. (A.9) is different from (35) and includes coherent diffraction, $hA \to XA$, which cross section reads [22, 28],

$$\sigma_{sd}^{hA}(hA \to XA) = \int d^2b \left\{\left\langle \exp\left[-\sigma_{tot}\,T_A^h(b)\right]\right\rangle \ - \left\langle \exp\left[-\frac{1}{2}\,\sigma_{tot}\,T_A^h(b)\right]\right\rangle^2\right\} \tag{37}$$

Averaging of the quasi-elastic cross section Eq. (A.13) leads to inclusion of diffractive excitation of the hadron $h \to X$ besides excitation of the nucleus, $A \to Y$.

Thus, Eq. (36) resulting from a direct averaging of the single channel inelastic cross section Eq. (A.14) corresponds to the part of the total hA cross section which does not contain, elastic scattering, $hA \to hA$, coherent diffraction, $hA \to XA$, quasi-elastic, $hA \to hY$, and double diffraction, $hA \to XY$. This part of the cross section is what is measured as the inelastic cross section in heavy ion and $p(d)A$ collisions at SPS and RHIC, and what we are going to calculate below.

One may wonder, what is the difference between the cross sections Eqs. (34)-(36) and those in Glauber approximation, Eqs. (A.5), (A.9) and (A.14)? The difference is obvious,

in the former set of equations the exponentials are averaged, while in the Glauber approximation contains exponentials of averaged values. For instance, the total cross section in the Glauber approximation reads,

$$\sigma_{tot}^{hA}\Big|_{Gl} = 2\int d^2b\left\{1-\exp\left[-\frac{1}{2}\left\langle\sigma_{tot}^{i}\right\rangle T_A^h(b)\right]\right\}\ , \tag{38}$$

where $\langle\sigma_{tot}\rangle = \sigma_{tot}^{hN}$. If to subtract this from Eq. (34), the rest is the Gribov's inelastic correction calculated in all orders. Indeed, we can compare it with the expression Eq. (34) expanding the exponentials in (34) and (38) in multiplicity of interactions up to the lowest order. Employing (33) we find,

$$\sigma_{tot}^{hA}-\sigma_{tot}^{hA}\Big|_{Gl} = \int d^2b\,\frac{1}{4}\left[\langle\sigma_{tot}^{i}\rangle^2-\langle(\sigma_{tot}^{i})^2\rangle\right]T_A^h(b)^2 = -4\pi\int d^2b\,T_A^h(b)^2\int dM^2\,\frac{d\sigma_{sd}^{h}}{dM^2dt}\Big|_{t=0}\ . \tag{39}$$

This result is identical to Eq. (26), if to neglect there the phase shift vanishing at high energies, and also to expand the exponential.

Note that since the inelastic nuclear cross section in the form Eq. (A.14) is correct for eigenstates, one may think that averaging this expression would give the correct answer. However, such a procedure includes possibility of excitation of the projectile and disintegration of the nucleus to nucleons, but misses possibility of diffractive excitation of bound nucleons which is not a small correction. We introduce a corresponding correction in the next section.

5 Light-cone dipoles and inelastic shadowing

5.1 Excitation of the valence quark skeleton

The light-cone dipole representation in QCD was introduced in [28] where it was realized that color dipoles are the eigenstates of interaction and can be an effective tool for calculation of diffraction and nuclear shadowing. It was concluded that the key quantity of the approach, the cross section of the dipole-nucleon, $\sigma_{\bar{q}q}^{N}(r_T)$, is a universal and flavor independent function which depends only on transverse separation r_T and energy. Of course the energy must be sufficiently high to freeze variations of the dipole size during interaction, otherwise one should rely on the Green function approach [20, 21, 29] (see Sect. 6).

This representation suggests an effective way to sum up all multi-step inelastic corrections in all orders [28]. Since dipoles are eigenstates of interaction in QCD, they are not subject to any diffractive excitation, and the eikonal approximation becomes exact. Therefore, if energy is high enough to keep the transverse size of a dipole "frozen" by Lorentz time dilation during propagation through the nucleus, one can write the cross sections in the form Eqs. (34)-(36). The averaging in this case means summing-up different Fock components of the hadron consisted of different numbers of quarks and gluons, and for each of them integration over r_T (intrinsic separations), weighted with the square of the hadron light-cone wave function $|\Psi_h(r_T)|^2$. We assume that the hadron does not have a "molecular" structure, i.e. is not like a deuteron consisting of two colorless clusters. Therefore all following

expressions apply only to elementary hadrons. To simplify calculations, in what follows we rely on the quark-diquark model of the proton, neglecting the diquark size. The total cross section is basically insensitive to the diquark size, besides, there are many evidences that this size is indeed small [30, 31].

5.1.1 Nuclear transparency

According to the Glauber model hadrons attenuate exponentially in nuclear matter,

$$Tr = \exp(-\sigma_{tot}^{hN}\, T_A)\ , \tag{40}$$

where Tr, called nuclear transparency, is the survival probability of a hadron propagating through a nuclear matter of thickness T_A. However, we know that the hadron fluctuates and can be viewed as a combination of Fock states of different content and size. Some of them having a small transverse size can easily penetrate the medium and do not attenuate as fast as in (40).

Assuming that the hadronic wave function has a Gaussian form and the dipole cross section $\sigma(r_T) \propto r_T^2$ (this small-r_T behavior does a good job describing hierarchy of hadronic cross sections and their sizes [32]) we can perform averaging in (34) and arrive at a rather simple expression [28],

$$\left\langle \exp[-\sigma(r)\, T_A] \right\rangle = \frac{1}{1+\sigma_{tot}^{hN}\, T_A}\ . \tag{41}$$

This explicitly demonstrates how Gribov's corrections make nuclei more transparent. Since exponential attenuation is much stronger than a power, for large T_A (central collisions with heavy nuclei) the difference might be tremendous.

5.1.2 Cross sections

.

The total cross section.

The total hadron-nucleus cross section is modified according to (41) as,

$$\sigma_{tot}^{hA} = \int d^2b\ \frac{\sigma_{tot}^{hN}\, T_A^h(b)}{1+\frac{1}{2}\sigma_{tot}^{hN}\, T_A^h(b)}\ ; \tag{42}$$

Although the Gribov's corrections (color transparency) make nuclei much more transparent, the modified total cross section Eq. (42) is not much smaller than the result of Glauber approximation Eq. (A.5). This is because the central area of a heavy nucleus is "black", i.e. fully absorptive, in both cases, and the cross section is mainly related to the geometry of the nucleus. In other words, the exponential term in (A.5) is very small for central collisions, and the total cross section is rather insensitive to even dramatic variations of its magnitude.

The elastic cross section

The partial elastic cross section is given by the square of the averaged value of the elastic amplitude. We get,

$$\sigma_{el}^{hA} = \frac{1}{4}\int d^2b\ \frac{[\sigma_{tot}^{hN}\,T_A^h(b)]^2}{[1+\frac{1}{2}\sigma_{tot}^{hN}\,T_A^h(b)]^2}\ . \tag{43}$$

Correspondingly, the differential elastic cross section reads,

$$\frac{d\sigma_{el}^{hA}}{dq_T^2} = \frac{1}{16\pi}\left|\int d^2b\ \frac{\sigma_{tot}^{hN}\,T_A^h(b)}{1+\frac{1}{2}\sigma_{tot}^{hN}\,T_A^h(b)}\ \exp(i\vec{q}\cdot\vec{b})\right|^2\ . \tag{44}$$

The total inelastic cross section

The cross section of all inelastic channels is given by the difference,

$$\sigma_{in}^{hA} = \sigma_{tot}^{hA} - \sigma_{el}^{hA} = \int d^2b\ \frac{\sigma_{tot}^{hN}\,T_A^h(b)\left[1+\frac{1}{4}\sigma_{tot}^{hN}\,T_A^h(b)\right]}{\left[1+\frac{1}{2}\sigma_{tot}^{hN}\,T_A^h(b)\right]^2}\ . \tag{45}$$

This cross section approaches the unitarity limit for $\sigma_{tot}^{hN}\,T_A^h(b) \gg 1$ at the nuclear center, but is proportional to $T_A^h(b)$ at the nuclear periphery.

Diffractive excitation of the hadron.

The combined cross section of elastic scattering and diffraction when the hadron may be either excited or not, but the nucleus remains intact, is given by the average of the dA elastic partial amplitude squared,

$$\sigma_{sd+el}^{hA}(hA\to XA) = \frac{1}{2}\int d^2b\ \frac{[\sigma_{tot}^{hN}\,T_A^h(b)]^2}{[1+\sigma_{tot}^{hN}\,T_A^h(b)][1+\frac{1}{2}\sigma_{tot}^{hN}\,T_A^h(b)]}\ . \tag{46}$$

Here we firstly averaged over the quark coordinates in the nucleons, secondly, squared the result, and thirdly, subtracted the elastic dA cross section [compare with (37)].

Diffractive excitation of the nucleus.

The cross section of the reaction where the nucleus is diffractively excited, and the hadron either remains intact or is excited too, reads,

$$\sigma_{qel}^{hA}(hA\to XA^*) = \int d^2b\ \frac{2\,\tilde{\sigma}_{el}^{hN}\,T_A^h(b)}{[1+\sigma_{tot}^{hN}\,T_A^h(b)]^3}\ , \tag{47}$$

where

$$\tilde{\sigma}_{el}^{hN} = \sigma_{el}^{hN} + \sigma_{sd}^{hN}(hN\to XN)) + \sigma_{sd}^{hN}(hN\to hY)) + \sigma_{dd}^{hN}(hN\to XY))\ , \tag{48}$$

and σ_{sd}^{hN} is a cross section of single diffractive excitation of either the beam or the target; the double diffractive cross section σ_{dd}^{hN} corresponds to diffractive excitation of both.

Deriving Eq. (47) we made use of smallness of the elastic cross section and expanded the exponential. Higher orders of σ_{el}^{hN} are neglected, but the corrections are easy to calculate. We also neglected the small variation of the elastic slope of the dipole-nucleon cross section with r_T.

Eq. (47), as one can see from (48), takes into account possibility of diffractive excitation of the projectile. This is a direct consequence of the eigenstate approach. In addition, we

also included the possibility of diffractive excitation of bound nucleons in the target. Those excitations are not shadowed by multiple interactions in the nucleus, since all extra particles produced this way stay in the nuclear fragmentation region and do not break down the large rapidity gap structure of the event. Therefore, they may be incorporated into $\tilde{\sigma}_{el}^{hN}$ adding the two last terms. At $\sqrt{s} = 200\,\mathrm{GeV}$ single and double diffraction cross section are about equal, $\sigma_{sd}^{NN} \approx \sigma_{dd}^{NN} \approx 4\,\mathrm{mb}$ [12, 13], $\sigma_{el}^{NN} \approx 9\,\mathrm{mb}$, so $\tilde{\sigma}_{el}^{NN} \approx 21\,\mathrm{mb}$.

Diffractive reactions Eq. (47)-(48) do not produce any particles at central rapidities. Therefore, if one wants to calculate the part of the total hadron-nucleus cross section detected experimentally, one should subtract these diffractive contributions,

$$\begin{aligned} \tilde{\sigma}_{in}^{hA} &= \sigma_{tot}^{hA} - \sigma_{sd+el}^{hA}(hA \to XA) - \sigma_{qel}^{hA}(hA \to XA^*) \\ &= \int d^2b\, \frac{\sigma_{tot}^{hN}\, T_A^h(b)}{1 + \sigma_{tot}^{hN}\, T_A^h(b)} \left\{ 1 - \frac{2\,\tilde{\sigma}_{el}^{hN}/\sigma_{tot}^{hN}}{[1 + \sigma_{tot}^{hN}\, T_A^h(b)]^2} \right\} . \end{aligned} \tag{49}$$

Since pp cross section is used as a baseline for comparison, the same subtraction should be done in this case too,

$$\tilde{\sigma}_{in}^{pp} = \sigma_{tot}^{NN} - \tilde{\sigma}_{el}^{NN} , \tag{50}$$

what comes to about $\tilde{\sigma}_{in}^{pp} = 30\,\mathrm{mb}$ at $\sqrt{s} = 200\,\mathrm{GeV}$.

Then, the number of collisions at given impact parameter corrected for inelastic shadowing reads,

$$N_{coll}(b) = \frac{\tilde{\sigma}_{in}^{NN}}{\sigma_{tot}^{NN}} \Big[1 + \sigma_{tot}^{NN}\, T_A^h(b) \Big] \left\{ 1 - \frac{\tilde{\sigma}_{el}^{NN}/\sigma_{tot}^{NN}}{[1 + \sigma_{tot}^{NN}\, T_A^h(b)]^2} \right\}^{-1} . \tag{51}$$

5.2 Deuteron-nucleus collisions

So far we considered the case of a colorless hadrons, but colored constituents. The specifics of a deuteron is that it contains two colorless clusters, nucleons. Therefore, one of the inelastic corrections which we already took into account in (7) is related to fluctuations of the deuteron size. The next step is to average over the fluctuations of the sizes of the nucleons.

The total deuteron-nucleus cross section.
Now we should average σ_{tot}^{dA} over the inter-nucleon separation, as well as over the nucleon sizes, $\vec{r}_1$ and $\vec{r}_2$,

$$\sigma_{tot}^{dA} = 2 \int d^2b \int d^2r_T \left| \Psi_d(r_T) \right|^2 \left\langle f^{dA}(\vec{b}, \vec{r}_T) \right\rangle_{r_1, r_2} , \tag{52}$$

where

$$\begin{aligned} \left\langle f^{dA}(\vec{b}, \vec{r}_T) \right\rangle_{r_1, r_2} &= 1 - \frac{1}{[1 + \frac{1}{2}\,\sigma_{tot}^{NN}\, T_A^N(\vec{b} + \frac{1}{2}\,\vec{r}_T)][1 + \frac{1}{2}\,\sigma_{tot}^{NN}\, T_A^N(\vec{b} - \frac{1}{2}\,\vec{r}_T)]} \\ &- \frac{\sigma_{el}^{NN}\, T_A^N(b)\, \exp\left(-\frac{r_T^2}{4B_{NN}} \right)}{[1 + \frac{1}{2}\,\sigma_{tot}^{NN}\, T_A^N(\vec{b} + \frac{1}{2}\,\vec{r}_T)]^2 [1 + \frac{1}{2}\,\sigma_{tot}^{NN}\, T_A^N(\vec{b} - \frac{1}{2}\,\vec{r}_T)]^2} . \end{aligned} \tag{53}$$

The result of calculation exposed in Table 1 is smaller than the Glauber model value. The difference comes from inelastic shadowing related to diffractive excitations of the colorless clusters in the deuteron, each consisted of three valence quarks.

Elastic and diffractive scattering of deuterons.
Correspondingly, the total cross section of elastic scattering and diffractive excitation of the deuteron has the form,

$$\sigma_{el}^{dA} + \sigma_{sd}^{dA}(dA \to XA) = \int d^2b \int d^2r_T \left|\Psi_d(r_T)\right|^2 \left\langle g^{dA}(\vec{b},\vec{r}_T)\right\rangle_{r_1,r_2} , \tag{54}$$

where

$$\begin{aligned}
\left\langle g^{dA}(\vec{b},\vec{r}_T)\right\rangle_{r_1,r_2} &= 1 - \frac{2}{[1+\frac{1}{2}\,\sigma_{tot}^{NN}\,T_A^N(\vec{b}+\frac{1}{2}\,\vec{r}_T)][1+\frac{1}{2}\,\sigma_{tot}^{NN}\,T_A^N(\vec{b}-\frac{1}{2}\,\vec{r}_T)]} \\
&+ \frac{2\,\sigma_{el}^{NN}\,T_A^N(b)\,\exp\left(-\frac{r_T^2}{4B_{NN}}\right)}{[1+\sigma_{tot}^{NN}\,T_A^N(\vec{+}\vec{r}_T)]^2[1+\sigma_{tot}^{NN}\,T_A^N(\vec{b}-\frac{1}{2}\,\vec{r}_T)]^2} \\
&+ \frac{1}{[1+\sigma_{tot}^{NN}\,T_A^N(\vec{b}+\vec{r}_T)][1+\frac{1}{2}\,\sigma_{tot}^{NN}\,T_A^N(\vec{b}-\frac{1}{2}\,\vec{r}_T)]} \\
&- \frac{2\,\sigma_{el}^{NN}\,T_A^N(b)\,\exp\left(-\frac{r_T^2}{4B_{NN}}\right)}{[1+\sigma_{tot}^{NN}\,T_A^N(\vec{b}+\frac{1}{2}\,\vec{r}_T)]^2[1+\sigma_{tot}^{NN}\,T_A^N(\vec{b}-\frac{1}{2}\,\vec{r}_T)]^2} .
\end{aligned} \tag{55}$$

Inelastic deuteron-nucleus collisions.
If to subtract the elastic and diffractive cross section Eq. (54) from (52) the rest will be the inelastic cross section which covers all diffractive excitations of the nucleus, but not gold. This is what is measured at the STAR experiment. To comply with the condition of experiments insensitive to diffraction one should also subtract the cross section of diffractive excitation of the nucleus. The results read [compare with (49)],

$$\begin{aligned}
\tilde{\sigma}_{in}^{dA} &= \sigma_{tot}^{dA} - \sigma_{el}^{dA} - \sigma_{sd}^{dA}(dA \to XA) - \sigma_{sd}^{dA}(dA \to dY) - \sigma_{dd}^{dA}(dA \to XY) \\
&= \int d^2b \int d^2r_T \left|\Psi_d(r_T)\right|^2 \left\langle h^{dA}(\vec{b},\vec{r}_T)\right\rangle_{r_1,r_2} ,
\end{aligned} \tag{56}$$

where

$$\begin{aligned}
\left\langle h^{dA}(\vec{b},\vec{r}_T)\right\rangle_{r_1,r_2} &= \left\{ 1 - \frac{1}{[1+\sigma_{tot}^{NN}\,T_A^N(\vec{b}+\frac{1}{2}\vec{r}_T)][1+\sigma_{tot}^{NN}\,T_A^N(\vec{b}-\frac{1}{2}\,\vec{r}_T)]} \right. \\
&- \frac{2\,\tilde{\sigma}_{el}^{NN}\,T_A^N(\vec{b}+\frac{1}{2}\,\vec{r}_T)}{[1+\sigma_{tot}^{NN}\,T_A^N(\vec{b}+\frac{1}{2}\,\vec{r}_T)]^3[1+\sigma_{tot}^{NN}\,T_A^N(\vec{b}-\frac{1}{2}\,\vec{r}_T)]} \\
&- \frac{2\,\tilde{\sigma}_{el}^{NN}\,T_A^N(\vec{b}-\frac{1}{2}\,\vec{r}_T)}{[1+\sigma_{tot}^{NN}\,T_A^N(\vec{b}+\frac{1}{2}\,\vec{r}_T)][1+\sigma_{tot}^{NN}\,T_A^N(\vec{b}-\frac{1}{2}\,\vec{r}_T)]^3} \\
&- \left. \frac{2\,\sigma_{el}^{NN}\,T_A^N(b)\,\exp\left(-\frac{r_T^2}{4B_{NN}}\right)}{[1+\sigma_{tot}^{NN}\,T_A^N(\vec{b}+\frac{1}{2}\,\vec{r}_T)]^2[1+\sigma_{tot}^{NN}\,T_A^N(\vec{b}-\frac{1}{2}\,\vec{r}_T)]^2} \right\} .
\end{aligned} \tag{57}$$

The results of calculations of both inelastic cross sections with and without nuclear diffraction, as well as the corresponding numbers collisions which are rather small compared to what was calculated in [1], are presented in Table 1. As expected, the cross sections are smaller than predicted by the Glauber model, while the numbers of collisions are larger. We also plotted b-dependence of σ_{in}^{dA} in Fig. 2 (thin solid curve). Comparing with the Glauber curve we see that this class of inelastic shadowing corrections leave the mid of nucleus "black", but makes it rather transparent on the periphery.

Production of spectator nucleons.
Similarly, one derives an equation for the cross section of a channel with tagged spectator nucleons corrected for inelastic shadowing,

$$\sigma_{tagg}^{dAu} = \int d^2b \int d^2r_T \, \frac{\left|\Psi_d(r_T)\right|^2}{1+\sigma_{tot}^{NN}\, T_A^N(\vec{b}+\frac{1}{2}\vec{r}_T)} \left\{ 1 - \frac{1}{1+\sigma_{tot}^{NN}\, T_A^N(\vec{b}-\frac{1}{2}\vec{r}_T)} - \frac{2\,\tilde{\sigma}_{el}^{NN}\, T_A^N(\vec{b}-\frac{1}{2}\vec{r}_T) + 2\,\sigma_{el}^{NN}\, T_A^N(b)\, \exp[-r_T^2/4B_{NN}]}{\left[1+\sigma_{tot}^{NN}\, T_A^N(\vec{b}+\frac{1}{2}\vec{r}_T)\right]^3} \right\}. \quad (58)$$

Events with tagged nucleons are especially sensitive to the transparency of the nucleus. We calculated the cross section, Eq. (58), and the results, as well as the corresponding numbers of collisions are shown in Table 1. The effect of inelastic corrections on the impact parameter distribution of interacting protons in tagged events with a spectator neutron is demonstrated in Fig. 3. Calculation was done for inelastic proton interaction including diffractive excitations (STAR). As one could anticipate, the nucleus becomes much more transparent in the center. Indeed, for a nearly black nucleus inelastic corrections keep it black since transparency, or the exponential term is so small that even if it is modified by a large factor, the final change is very small. However, tagged events is a direct measure of transparency, and the inelastic corrections are maximal in this case. It is not surprising that N_{coll} is quite large (considering that only one nucleon interacts.

5.3 Towards realistic calculations

5.3.1 Three valence quarks

.

For the sake of simplicity we used so far the approximation of a quark-diquark structure of the proton, and neglected the diquark size. As long as the diquark is indeed as small as $0.2-0.3\,\mathrm{fm}$ [30, 31], this approximation is rather precise even for heavy nuclei which hardly can resolve such a small size. However, the mean size of the isoscalar diquark is still a debatable issue, besides, an isovector diquark is probably a big object. Then, one may expect nuclear matter to be more opaque for a high energy nucleon compared to what was found above.

We evaluate nuclear transparency for another extreme, i.e. for the case of a proton wave function symmetric in all quark coordinates, with a mean size of any diquark of the order

of 0.7 fm,

$$|\Psi_N(\vec{r}_1,\vec{r}_2,\vec{r}_3)|^2 = \frac{3}{(\pi\, r_N^2)^2}\exp\left(-\frac{r_1^2+r_2^2+r_3^2}{r_N^2}\right)\,\delta(\vec{r}_1+\vec{r}_2+\vec{r}_3)\ . \tag{59}$$

To perform the averaging of the eikonal exponentials in (34)-(36) we need to know the three-body dipole cross section, which we express via the conventional $\bar{q}q$ one as,

$$\sigma_{3q}(\vec{r}_1,\vec{r}_2,\vec{r}_3) = \frac{1}{2}\left[\sigma_{\bar{q}q}(r_1)+\sigma_{\bar{q}q}(r_2)+\sigma_{\bar{q}q}(r_3)\right]\ . \tag{60}$$

It satisfies the limiting conditions, namely, turns into $\sigma_{\bar{q}q}(r)$ if one of three separations is zero. Assuming that $\sigma_{\bar{q}q}(r) = Cr^2$, this cross section averaged with the wave function squared Eq. (59) gives $\sigma_{tot}^{NN} = Cr_N^2/2$.

Now we can calculate the nuclear transparency averaging the eikonal exponential,

$$\begin{aligned}\left\langle \exp\left[-\sigma_{3q}(r_i)T_A(b)\right]\right\rangle &= \int\prod_i^3 d^2r_i\ |\Psi_N(\vec{r}_1,\vec{r}_2,\vec{r}_3)|^2\ \exp\left[-\sigma_{3q}(\vec{r}_1,\vec{r}_2,\vec{r}_3)\,T_A(b)\right]\\ &= \frac{1}{\left[1+\frac{1}{2}\,\sigma_{tot}^{NN}\,T_A(b)\right]^2}\end{aligned} \tag{61}$$

We see that nuclear transparency in this case is quadratic, rather than linear function of the inverse nuclear thickness. For small $\sigma_{tot}^{NN}\,T_A(b) \ll 1$ it coincides with the result of the quark-diquark model, Eq. (41), however falls steeper at large $T_A(b)$. This is not surprising: in order to make use of color transparency the whole proton has to fluctuate into a small transverse area, and it is more probable for a two- than three-body system.

One can consider these results as a lower [Eq. (61)] and an upper [Eq. (41)] bound for nuclear transparency. We calculated different cross sections using the average of the eikonal exponential in the form Eq. (61) instead of Eq. (41), and the results are shown in Table 1 in parenthesis. Unfortunately, we still do not know the proton wave function sufficiently well to fix this uncertainty for nuclear transparency. Nevertheless, the difference is not large for real nuclei. For instance, the inelastic non-diffractive $d-Au$ cross section presented in Table 1 increases by about 6%.

5.3.2 Realistic dipole cross section

.

The dipole cross section $\sigma_{\bar{q}q}^N \propto r_T^2$ used above is justified only for small r_T, while it is expected to level off at large $\bar{q}q$ separations. More reliable calculations can be done using a realistic phenomenological cross section. A quite popular parametrization was proposed in [33] and fitted to HERA data for $F_2(x,Q^2)$. However, it should not be used for our purpose, since is unable to provide the correct energy dependence of hadronic cross sections. Namely, the pion-proton cross section cannot exceed 23 mb [5].

[5] According to [34] this dipole cross section reproduced well the energy dependence of the photoabsorption cross section $\sigma_{tot}^{\gamma p}(s)$. This happens only due to the singularity in the light-cone wave function of the photon at small r_T. This is a specific property of the transverse photon wave function and is not applicable to hadrons.

A parametrization more appropriate for soft hadronic physics was proposed in [11]:

$$\sigma_{\bar{q}q}(r_T,s)=\sigma_0(s)\,\left[1-\exp\left(-\frac{r_T^2}{R_0^2(s)}\right)\right]\,, \tag{62}$$

where $R_0(s)=0.88\,fm\,(s_0/s)^{0.14}$ and $s_0=1000\,GeV^2$. In contrast to [33] all values depend on energy (as it is supposed to be for soft interactions) rather than on x and the energy dependent parameter $\sigma_0(s)$ is defined as,

$$\sigma_0(s)=\sigma_{tot}^{\pi p}(s)\,\left(1+\frac{3\,r_0^2(s)}{8\,\langle r_{ch}^2\rangle_\pi}\right)\,, \tag{63}$$

Here $\langle r_{ch}^2\rangle_\pi=0.44\pm0.01\,fm^2$ [35] is the mean square of the pion charge radius. Cross section (62) averaged with the pion wave function squared automatically reproduces the pion-proton cross section. The pp total cross section is also well reproduced using the quark-diquark approximation for the proton wave function. The parameters are adjusted to HERA data for the proton structure function. Agreement is quite good up to at least $Q^2\sim 10\,GeV^2$ sufficient for our purposes.

With such a dipole cross section one can perform analytic calculations expanding the Glauber exponentials in (34)-(37). Then the total cross section gets the form,

$$\sigma_{tot}^{hA}=2\int d^2b\,\left\{1-\exp\left[-\frac{1}{2}\sigma_0(s)T_A^h(b)\right]\sum_{n=0}^{\infty}\frac{[\sigma_0(s)T_A^h(b)]^n}{2^n\,n!\,(1+n\,\delta)}\right\}\,; \tag{64}$$

Correspondingly, the sum of elastic and diffractive deuteron scattering on the nucleus reads,

$$\begin{aligned}\sigma_{sd+el}^{hA}(hA\to XA) &= \int d^2b\,\left\{1+\exp\left[-\frac{1}{2}\sigma_0(s)T_A^h(b)\right]\right.\\ &\times \left.\sum_{n=0}^{\infty}\frac{[\sigma_0(s)T_A^h(b)]^n}{n!\,(1+n\,\delta)}\,\left(1-2^{1-n}\exp\left[-\frac{1}{2}\sigma_0(s)T_A^h(b)\right]\right)\right\}\,.\end{aligned} \tag{65}$$

The cross section of quasielastic excitation of the nucleus with simultaneous possibility to excite the deuteron is given by,

$$\begin{aligned}\sigma_{qel}^{hA}(hA\to XA^*) &= \int d^2b\,\exp\left[-\frac{1}{2}\sigma_0(s)T_A^h(b)\right]\\ &\times \sum_{n=0}^{\infty}\frac{[\sigma_0(s)\,T_A^h(b)]^n}{n!}\,\frac{2\delta^2}{[1+n\delta][1+(n+1)\delta][1+(n+2)\delta]}\,.\end{aligned} \tag{66}$$

In all these equations

$$\delta=\frac{8\langle r_p^2\rangle}{3R_0^2(s)}\,. \tag{67}$$

Now one can calculate $\tilde{\sigma}_{in}^{hA}$ subtracting (65) and (66) from (64). However, in this paper we restrict ourselves by calculations performed above and leave this more complicated computation for further study.

6 Gluon shadowing and the triple-Pomeron diffraction

First of all, to avoid confusion it should be emphasized that we are not talking about gluon shadowing in high-p_T hadron production at $x_F = 0$ in $d - Au$ collisions. This process exploits Bjorken $x > 0.01$ which are too large for gluon shadowing [4, 11]. On the contrary, we consider gluon shadowing in the soft inelastic $d - Au$ collisions which are the main contributor to the total cross section. This process is related to much smaller $x \sim 10^{-5}$.

Gluon shadowing is an important source of inelastic corrections at very high energies. It is pretty clear if one employs Eq. (26). The part of the diffraction which corresponds to the triple-Regge graph $I\!P I\!P I\!R$, or the lowest order Fock component consisted only of valence quarks, has a steep M-dependence, $d\sigma_{sd}^{hN}/dM^2 \propto 1/M^3$. Therefore the integral over M^2 in (26) well converges, the minimal momentum transfer q_L vanishes at high energies, and this part of inelastic corrections saturates.

The triple-Pomeron ($I\!P I\!P I\!P$) part of diffraction which corresponds to the Fock state containing at least one gluon, is divergent at large masses, $d\sigma_{sd}^{hN}/dM^2 \propto 1/M^2$, since the gluon is a vector particle. The cut off is imposed by the nuclear formfactor in (26), i.e. the condition $q_L \lesssim 1/R_A$. As a result of the divergence, this part of the inelastic corrections rises as $\ln(s/s_0)$ and reaches a substantial value at the energy of RHIC.

Eikonalization of the lowest Fock state $|3q\rangle$ of the proton done in (34)-(36) corresponds to the Bethe-Heitler regime of gluon radiation. Indeed, gluon bremsstrahlung is responsible for the rising energy dependence of the phenomenological cross section (62), and in the eikonal form (34)-(36) one assumes that the whole spectrum of gluons is multiply radiated. However, the Landau-Pomeranchuk-Migdal (LPM) effect [36, 37] is known to suppress radiation in multiple interactions. Since the main part of the inelastic cross section at high energies is related to gluon radiation, the LPM effect becomes a suppression of the cross section. This is a quantum-mechanical interference phenomenon and it is a part of the suppression called Gribov's inelastic shadowing. The way how it is taken into account in the QCD dipole picture is inclusion of higher Fock states, $|3qG\rangle$, etc. Each of these dipoles is of course colorless and its elastic amplitude on a nucleon is subject to eikonalization.

As already mentioned, Eq. (26) should not be used at high energies as it misses all higher order multiple off-diagonal transitions, and incorrectly (ad hoc) calculates diagonal ones. On the other hand, the eigenstate expressions Eqs. (34)-(36) is not safe to use either. Indeed, the significant part of the integral over M^2 in (26), next to the upper cut off, corresponds to a finite q_L. In other words, the fluctuation *valence quarks + gluons* is not frozen by Lorentz time dilation during propagation through the nucleus.

6.1 The Green function for glue-glue dipoles

A proper treatment of a quark-gluon fluctuation "breathing" during propagation through a nucleus is offered by the light-cone Green function formalism. In this approach the absorption cross section, as well as the phase shifts, are functions of longitudinal coordinate. This is also a parameter-free description, all the unknowns are fixed by the comparison with other data. We employ this approach and calculate gluon shadowing following Ref. [11].

The key point which affects the further calculations is the nonperturbative light-cone

wave function of the quark-gluon Fock state,

$$\Psi_{qG}(\vec{r}) = \frac{2}{\pi}\sqrt{\frac{\alpha_s}{3}}\,\frac{\vec{e}\cdot\vec{r}}{r^2}\exp\left(-\frac{r^2}{2r_0^2}\right)\ . \tag{68}$$

Here we assume (as usual) that the gluon is carrying a negligible fraction, $\alpha_G \ll 1$, of the quark momentum. This wave function is quite different from the perturbative one which is the same as in light-cone description of the Drell-Yan process [11, 38]. The latter, employed for calculation of diffractive gluon radiation (the triple-Pomeron term), results in overestimation of data for large mass diffraction more than by order of magnitude. This problem has been known since the 70s as the puzzle of smallness of the triple-Pomeron coupling. The way out is to make a natural assumption that the parent light-front quark and gluon experience a nonperturbative interaction which squeezes that quark-gluon wave packet, and therefore reduces the dipole cross section. The parameter r_0 in (68) controls the strength of the real part of the light-cone potential which is chosen in a Gaussian form. Fit to diffractive data $pp \to pX$ leads to the value of the mean transverse $q-G$ separation $\sqrt{\langle r^2\rangle} \equiv r_0 = 0.3\,\mathrm{fm}$. This conclusions goes along with the results of nonperturbative models, like the instanton vacuum model [39], and lattice calculations [40], which found a similar small size for gluonic fluctuations. Such a semihard scale, $1/r_0$ also leads to quite a steep energy behavior of the radiation cross section and well explains data for the total and differential elastic cross sections of pp scattering [41].

Apparently, smallness of r_0 leads to quite a weak shadowing for Fock states containing gluons. As a consequence, we expect rather weak gluon shadowing, what is not a surprise in view of the close connection between diffraction and shadowing. As long as the gluon clouds around valence quarks small, the Gribov's corrections are suppressed. Besides the fluctuations containing gluons become heavy and the onset of gluon saturation takes place at much smaller x than usually expected.

The mean quark-gluon separation $r_0 \approx 0.3\,fm$ is much smaller than the quark separation in light hadrons. For this reason one can neglect the interferences between the amplitudes of gluon radiation by different valence quarks. Since the gluon contribution to the cross section corresponds to the difference between the amplitudes of $|qqqG\rangle$ and $|qqq\rangle$ components, the spectator quarks cancel out. Then the radiation cross section is controlled by the quark-gluon wave function and color octet (GG) dipole cross section.

Thus, the contribution to the total hadron-nucleus cross section which comes from gluon radiation has the form,

$$\sigma_G^{hA} = \int_x^1 \frac{d\,\alpha_G}{\alpha_G}\int d^2b\,P(\alpha_G,\vec{b})\ , \tag{69}$$

where α_G is the fraction of the quark momentum carried by the gluon;

$$\begin{aligned} P(\alpha_G,\vec{b}) &= T_A(b)\int d^2r\left|\Psi_{qG}(\vec{r},\alpha_G)\right|^2\sigma_{GG}(r,s) \\ &- \frac{1}{2}\,\mathrm{Re}\int_{-\infty}^{\infty} dz_1\,dz_2\,\Theta(z_2-z_1)\,\rho_A(b,z_1)\,\rho_A(b,z_2)\int d^2r_1\,d^2r_2 \\ &\times \Psi^*_{qG}(\vec{r}_2,\alpha_G)\sigma_{GG}(r_2,s)\,G_{GG}(\vec{r}_2,z_2;\vec{r}_1,z_1)\,\sigma_{GG}(r_1,s)\,\Psi_{qG}(\vec{r}_1,\alpha_G)\ . \end{aligned} \tag{70}$$

Here the energy and Bjorken x are related as $s = 2m_N E_q = 4/xr_0^2$.

The second term in (70) corresponds to the triple-Pomeron part of the inelastic correction Eq. (26) written in impact parameter representation. The amplitude of diffractive gluon radiation $qN \to GqN$ is proportional to $\Psi_{qG}(\vec{r}, \alpha_G)\sigma_{GG}(r)$. A glue-glue dipole emerges in this expression because this is not elastic scattering, but a production process. Its amplitude comes from the difference of the scattering amplitudes of different Fock components of the quark [38], $|q\rangle$ and $|qG\rangle$, which is a dipole cross section of a color octet-octet dipole, $\bar{q}q - G$. Since the size of the $\bar{q}q$ pair is irrelevant for gluon shadowing, we neglect it and replace the $\bar{q}q$ by a gluon (see in [11, 42]). Therefore the second term in (70) can be interpreted as production of a qG pair at the point z_1, then propagation of this pair with varying transverse separation up to point z_2 where it converts back to the quark.

Propagation of the dipole of varying size through the absorptive medium between points z_1 and z_2 is described by the Green function $G_{GG}(\vec{r}_2, z_2; \vec{r}_1, z_1)$. It satisfies the two dimensional Schrödinger equation,

$$i\,\frac{d}{d\,z_2}\,G_{GG}(\vec{r}_2, z_2; \vec{r}_1, z_1) = \left[-\frac{\Delta(\vec{r}_2)}{2\,E_q\,\alpha_G(1-\alpha_G)} + V(\vec{r}_2, z_2)\right] G_{GG}(\vec{r}_2, z_2; \vec{r}_1, z_1)\ , \qquad (71)$$

where imaginary part of the light-cone potential is related to absorption in the medium,

$$\mathrm{Im}\,V(\vec{r}, z) = -\frac{1}{2}\,\sigma_{GG}(\vec{r})\,\rho_A(b, z)\ . \qquad (72)$$

For further calculations we assume that the quark energy is $E_q = s/6m_N$, but the results are hardly sensitive to this approximation.

Perturbative calculations treating a quark-gluon fluctuation as free particles overestimates the cross section of diffractive gluon radiation (or the triple-Pomeron coupling) more than by an order of magnitude. The only way to suppress this cross section is to reduce the mean transverse size of the fluctuation. This is done in [11] via introduction of a real part of the light-cone potential in (71),

$$\mathrm{Re}\,V(\vec{r}, z) = \frac{r^2}{2\,E_q\,r_0^4\,\alpha_G(1-\alpha_G)}\ , \qquad (73)$$

where parameter $r_0 =$ was fitted to data for single diffraction $pp \to pX$.

The gluonic dipole cross section $\sigma_{GG}(r, s)$ is assume to be different from the $\bar{q}q$ one, Eq. (62), only by the Cazimir factor 9/4. To simplify calculations we rely on the small-r approximation, $\sigma_{GG}(r, s) \approx C_{GG}(s)\,r^2$, where $C_{GG}(s) = d\,\sigma_{GG}(r, s)/d\,r^2_{r=0}$. This approximation for the dipole cross section is justified by the small value of $r_0^2 \approx 0.1\,fm^2$.

In the case of a constant nuclear density, $\rho_A(r) = \rho_A\,\Theta(R_A - r)$, the solution of Eq. (71) has a form,

$$\begin{aligned} G_{GG}(\vec{r}_2, z_2; \vec{r}_1, z_1) &= \frac{A}{2\pi\sinh(\Omega\,\Delta z)} \\ \times\quad \exp&\left\{-\frac{A}{2}\,\left[(r_1^2 + r_2^2)\coth(\Omega\,\Delta z) - \frac{2\vec{r}_1\cdot\vec{r}_2}{\sinh(\Omega\,\Delta z)}\right]\right\}\ , \end{aligned} \qquad (74)$$

where

$$\begin{aligned} A &= \frac{1}{r_0^2}\sqrt{1 - i\,\alpha_G(1-\alpha_G)\,E_q\,C_{GG}\,\rho_A\,r_0^4} \\ \Omega &= \frac{i\,A}{\alpha_G(1-\alpha_G)\,E_q} \\ \Delta z &= z_2 - z_1\ . \end{aligned} \tag{75}$$

Integrations in (70) can be performed analytically,

$$P(\alpha_G, \vec{b}) = \frac{4\,\alpha_G}{3\,\pi}\ \mathrm{Re}\,\ln(W)\ , \tag{76}$$

where

$$W = \cosh(\Omega\,L) + \frac{A^2 r_0^2 + 1}{2\,A}\ \sinh(\Omega\,L)\ , \tag{77}$$

$$L = 2\,\sqrt{R_A^2 - b^2}\ . \tag{78}$$

The first term in (70) is a part of the nuclear cross section calculated in Bethe-Heitler limit, i.e. without gluonic inelastic shadowing. Therefore it is included in the nuclear cross sections calculated so far. The new inelastic shadowing correction comes from the second term in (70). Its fraction of the total pA cross section is depicted in Fig. 8. The onset of

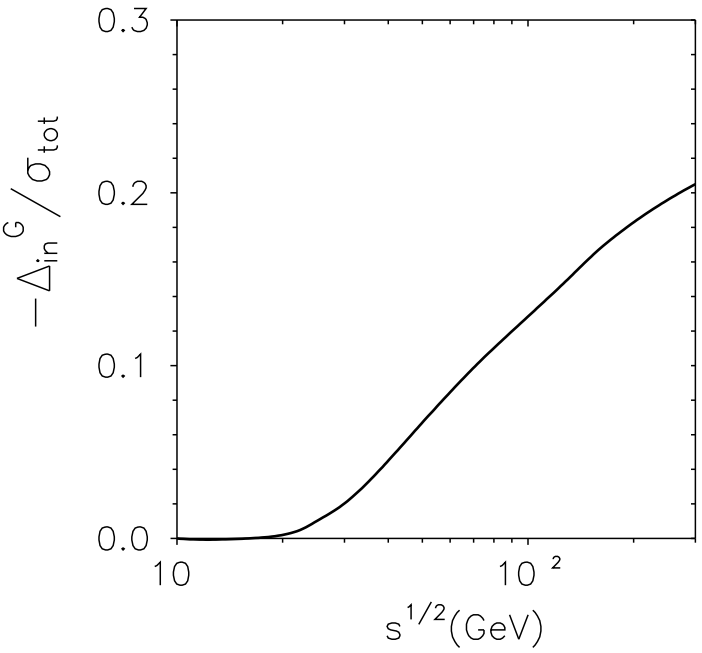

Figure 8: *Ratio of the gluonic inelastic shadowing correction (minimal bias) to the total nuclear cross section as function of c.m. energy* $\sqrt{s}$.

shadowing is delayed up to $\sqrt{s} \sim 20\,\mathrm{GeV}$. We believe that this result is trustable since the

Green function approach treats phase shifts and attenuation in nuclear matter consistently. Nevertheless, in order to get an idea about the scale of theoretical uncertainty we also evaluated the magnitude of gluon shadowing using the known values of the triple-Pomeron coupling and equation (26). The results are quite similar, in both cases the gluon shadowing correction is pretty small [11], $\sim 20\%$ at the energy of RHIC. Such a weak shadowing is a direct result of smallness of the parameter $r_0 = 0.3\,\mathrm{fm}$ which we use. This seems to be the only way to suppress diffractive gluon radiation corresponding to the triple-Pomeron contribution, and to reach agreement with data on diffractive dissociation $pp \to pX$. For this reason, all effects related to gluons, including saturation, or color-glass condensate, are quite suppressed.

Naturally, the inelastic correction in (70), (77) varies with impact parameter vanishing on the very periphery and reaching a maximum at central collisions. At small $T_A(b)$ the inelastic correction is proportional to $T_A^2(b)$ while the partial amplitude is proportional to $T_A(b)$. Therefore, the ratio linearly rises with $T_A(b)$ (see in [43, 44]) with a coefficient approximately equal to $0.2\,\mathrm{fm}^2$. For very large $T_A^2(b)$ the correction may even exceed the rest of the cross section, then apparently higher order corrections must be added to stop this growth. Such a saturation is not important for real nuclei, therefore we use the linear parametrization $R_G(b) = 1 - \Delta_{in}^G(b) = 1 - 0.2\,T_A(b)$ for further calculations.

The valence quark part of the inelastic shadowing corrections makes the nucleus more transparent, i.e. reduces the elastic scattering amplitude as one can explicitly see comparing the corrected amplitude Eq. (42) with the Glauber form Eq. (A.5). However, both approach the black disc limit for large $T_A(b)\sigma_{tot}^{NN} \gg 1$. Important question is whether this is still true after inclusion of gluonic corrections.

Eq. (70) has the typical form of a nonlinear equation like Glibov-Levin-Ryskin evolutions equation (GLR) [45], or in the dipole form Balitsky-Kovchegov equation (BK) [46]. The second term on the right-hand side of (70) corresponds to glue-glue fusion in GRL or the multiple interaction in the nucleus in BK equations. We calculated the correction in the lowest order using the uncorrected dipole cross section $\sigma_{GG}(r)$, i.e. the undisturbed free gluon density. Next iterations would be to implement the corrected gluon density (at larger x, however), or $\sigma_{GG}(r)$, into the second term in (70). This procedure leads to the BK equation which solution is still a challenge. However, due to smallness of the correction, 20%, we do not expect large higher order corrections and the saturated solution should not be very different from our result which we employ in further applications.

On the other hand, if gluon shadowing emerging from the first order iteration is very strong, like it was found in [47–49], it should be substantially reduced by next iterations which effectively play role of self-screening. Namely, as long as the gluon density is reduced at small x, one cannot use in Eq. (26) the cross section of diffractive dissociation on a free nucleon target. It is suppressed by the same gluon shadowing (at larger x though). The stronger is the gluon shadowing the more important is this self-screening effect. It was missed in calculations [47–49] which grossly over-predicted the strength of gluon shadowing.

Now we are in a position to correct our previous calculations for the gluonic part of inelastic shadowing which we fix at 20%. We do it replacing $\sigma_{\bar{q}q}(r_T) \Rightarrow R_G(b)\,\sigma_{\bar{q}q}(r_T)$, where $R_G(b) = 1 - \Delta_{in}(b)$ is the suppression factor related to gluon shadowing. This simple prescription is based on the intuitive expectation that a dipole interacts with a less number of

gluons in the nucleus than the eikonal model assumes. Indeed, for small separations r_T, the dipole cross section reads [50], $\sigma_{\bar{q}q}(r_T) = (\pi^2/3)\alpha_s\, r_T^2\, G(x, r_T)$, i.e. it is indeed proportional to the gluon density which is reduced in nuclei. More motivations for this procedure can be found in [43, 44].

The results for nuclear cross sections corrected for gluon shadowing are shown in Table 1 and depicted in Fig. 2-4 by thick solid curves.

6.2 More models for gluon shadowing

Although we predict quite a modest qluon shadowing effect and therefore a rather small inelastic shadowing correction, many models predict much stronger effects. One can call it theoretical uncertainty, if one treats all models equally (though some of them are probably more equal than others [51]).

For instance, the popular event generator HIJING contains a Q^2-independent gluon shadowing [52] which is a factor 0.3 at $x \sim 10^{-5}$. With such a dramatic gluon shadowing we get the impact parameter dependence of the inelastic cross section depicted by dotted curve in Fig. 2. The corresponding correction factor $K = 0.65$ for the PHENIX data.

If to treat shadowing in terms of the dipole approach, it is clear that shadowing is a monotonic function of Q^2, since the size of the dipole can only rise towards the soft limit. This is confirmed by DGLAP evolution of nuclear shadowing in the perturbative domain. Therefore, one can use gluon shadowing predicted by different models at the starting scale Q_0 of the order of $1 - 2\,\mathrm{GeV}^2$ as a bottom bound for the shadowing correction expected in the soft limit. We calculate Bjorken x for the RHIC energy $\sqrt{s} = 200\,\mathrm{GeV}$ and $Q^2 = 1\,\mathrm{GeV}^2$.

A strong gluon shadowing was predicted in [47, 48], $R_G = 0.3 - 0.4$. HERA data for diffraction $\gamma^* p \to Xp$ was used as an input in equation (26) modified for $\gamma^* A$ collisions. The statistics of this data is much lower than in proton diffraction $pp \to pX$ and not sufficient for reliable determination of the triple-Pomeron coupling. Different solutions for this coupling fitted to DIS diffractive data vary dramatically [53]. Besides, as is mentioned above, the gluon self-screening missed in [47, 48] should significantly reduce the effect of gluon shadowing.

Explicit calculations of gluon shadowing via gluon dipoles was performed in [49]. The gluon shadowing corresponding to the RHIC energies was found at $R_G \approx 0.6$ what leads to correction factor $K = 0.78$ for the Phenix ratio R_{dA}. This calculation, however, also does not include the gluon self screening, and is based on the assumption that gluon and quark dipoles have identical distribution functions.

A strong gluon suppression was also found in a model with an early onset of strong saturation [54] which characteristic scale is a steep function of energy, $Q_s^2 \propto (1/x)^{0.252}$. It was assumed in the KLM approach [6] that for $Q^2 \leq Q_S^2$ gluon density $xG_A(x, Q^2)$ is proportional to $Q^2\, R_A^2$ with a factor which was taken from the McLerran-Venugopalan model [55] at $x = 10^{-1}$. Such an oversimplified picture exhibits a strong gluon shadowing. If to compare the $xG_A(x, Q^2)$ with the GRV parametrization [56] at $x \sim 10^{-4}$ it turns out to be strongly suppressed by factor $R_G = 0.42$. In this case the correction factor in (5) is $K = 0.72$.

Such a diversity of model predictions suggests a conclusion that the current data for

deuteron-gold collisions [1–3] cannot resolve in a model independent way the dilemma, whether final state interaction or initial conditions is the main source of hadron suppression in heavy ion collisions. Indeed, if the latter were true, it would unavoidably lead to a substantial reduction of σ_{in}^{NA} and the ratio Eq. (5) (compared to the Glauber model).

6.3 Number of participants

Although the concept of number of participants originates from a naive treatment of multiparticle production called wounded nucleon model, it is a widely used characteristics of centrality of collisions. We are not going to dispute here its meaning, but just to see how it is affected by the inelastic corrections[6] relying on its formal definition,

$$\left.\frac{dN_p(s,b)}{d^2b}\right|_{Gl} = T_A(\vec{s}-\vec{b})\left\{1-\exp\left[-\sigma_{in}^{NN}\,T_B(b)\right]\right\} + T_B(s)\left\{1-\exp\left[-\sigma_{in}^{NN}\,T_A(\vec{s}-\vec{b})\right]\right\}\ , \tag{79}$$

where $\vec{s}$ is the parameter of collision of nuclei A, B. We use subscript Gl to emphasize that it corresponds to this model which is inspired by the Glauber model (although they have nothing in common).

Apparently, inelastic shadowing corrections should reduce N_p since nuclear matter becomes more transparent. The corrected expression for N_p reads,

$$\begin{aligned}\frac{dN_p(s,b)}{d^2b} &= \sigma_{in}^{NN}\,T_A(\vec{s}-\vec{b})\,T_B(b) \\ &\times \left\{\frac{R_G(b)}{1+R_G(b)\,\sigma_{in}^{NN}\,T_B(b)} + \frac{R_G(\vec{s}-\vec{b})}{1+R_G(\vec{s}-\vec{b})\,\sigma_{in}^{NN}\,T_A(\vec{s}-\vec{b})}\right\}\ .\end{aligned} \tag{80}$$

Here the gluon shadowing factor R_G is function of impart parameter according to calculations in [11, 43, 44] and the parametrization used above. We present the correction to the "Glauber" expression defines as,

$$\delta_{shad}(b) = \frac{R_G(b)\,\sigma_{in}^{NN}\,T_B(b)}{1+R_G(b)\,\sigma_{in}^{NN}\,T_B(b)}\Big/\left\{1-\exp\left[-\sigma_{in}^{NN}\,T_B(b)\right]\right\}\ , \tag{81}$$

in Fig. 9 depicted by solid curve. As one could expect, the correction factor peaks at the nuclear periphery and approaches one at large impact parameters.

If to compare with Glauber calculations employing the incorrect inelastic cross section $\sigma_{in}^{NN} = 42\,\mathrm{mb}$, the correction is even larger, as is demonstrated by dashed curve in Fig. 9.

7 Cronin effect: renormalizing the data

Cronin effect for high-p_T pions at $\sqrt{s} = 200\,\mathrm{GeV}$ was predicted in [4] to be a rather small enhancement, about 10% at the maximum. The smallness of the effect is due to the change of the mechanism of high-p_T particle production which takes place at the RHIC energies.

[6] I am thankful to Larry McLerran suggested to look at this parameter.

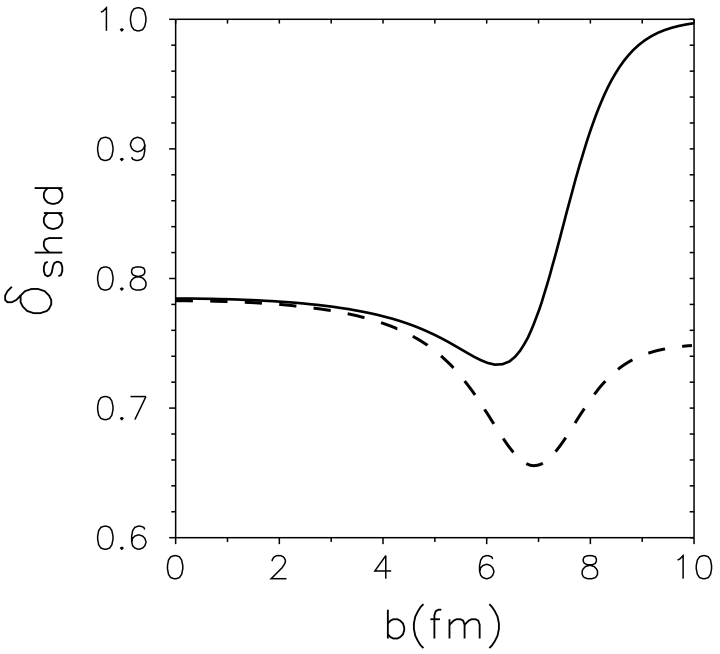

Figure 9: *Solid line is the correction factor Eq. (81) for inelastic shadowing to the number of participants in $p-Au$ collisions as function of impact parameter. Dashed curve also includes a correction to σ_{in}^{NN} (see text).*

At lower energies (SPS, CERN) different bound nucleons contribute to this hard process incoherently. The nuclear enhancement is due to initial/final state p_T-broadening of partons propagating through the nucleus. This broadening should not be translated into a modification of the parton distribution in the nucleus since k_T-factorization is broken [57]. At high energy an incoming light-cone fluctuation which contains a high-p_T parton is freed via coherent interaction with many nucleons in the target. It turns out that such a coherent mechanism leads to a weaker Cronin enhancement than the incoherent one. This is why calculations [58, 59] missing this effect of coherence, predict a stronger Cronin effect.

The PHENIX data for neutral pions [1] are depicted in Fig. 10 by full points in comparison with the predicted ratio [4]. However, as it was stressed above, the normalization of the data is based on Glauber model calculations which are subject to different corrections, all of which have negative sign. As a result, the data should be renormalized according to Table 1 by multiplying the experimental values by coefficient $K = 0.83$. The corrected data are shown by open circles.

Cronin effect on a deuteron

Theoretical predictions has been done so far for pA collisions. In order to compare models with dA data one should make sure that the Cronin enhancement on the deuteron

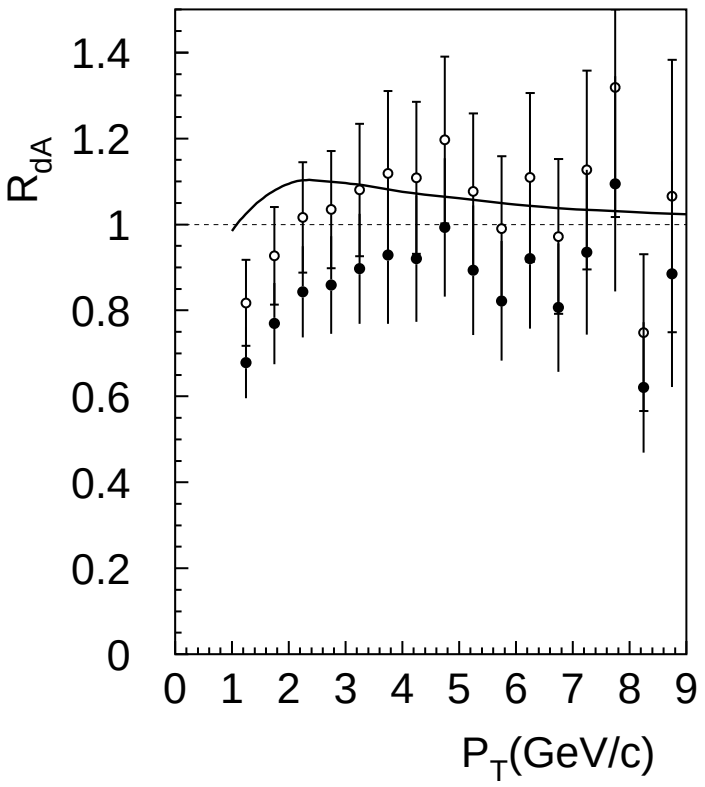

Figure 10: *The Cronin ratio $R_{Au/d}(p_T)$ for pions. Open circles show the results of PHENIX with normalization base upon Glauber model calculations of the inelastic $d-Au$ cross section using $\sigma_{in}^{NN} = 42\,mb$ [1]. Full points show the same data corrected for a proper value of inelastic NN cross section and Gribov's inelastic shadowing. The error bars includes statistic and systematic uncertainties. The curve is the prediction from [4].*

itself is a small corrections. We evaluate the ratio,

$$R_{pd}(p_T) = \frac{d\sigma^{pd}/d^2p_T}{2\,d\sigma^{pp}/d^2p_T}\ , \tag{82}$$

in the limit of short coherence length which gives an upper estimate for the effect. Following [4] the pd cross section at high p_T is given by the following convolution,

$$\sigma_{pd}(p_T) = \sum_{i,j,k,l} \widetilde{F}_{i/p} \otimes F_{j/d} \otimes \hat{\sigma}_{ij\to kl} \otimes D_{h/k}\ , \tag{83}$$

where $F_{i/p}$ and $F_{j/d}$ are the distributions of parton species i,j dependent on Bjorken $x_{1,2}$ and transverse momenta of partons in the colliding proton and deuteron respectively. The beam parton distribution $\widetilde{F}_i^p$ is modified by the transverse momentum broadening of the

projectile parton due to interaction with another nucleon in the deuteron. The broadening of the mean transverse momentum squared reads [60, 61],

$$\Delta\langle k_T^2\rangle = 2\ \frac{d\sigma_{\bar{q}q}(r_T)}{dr_T^2}\bigg|_{r_T=0}\ \langle T\rangle\ , \tag{84}$$

where $\langle T\rangle$ is the mean nuclear (deuteron) thickness covered by the projectile parton before or after the hard collision,

$$\langle T\rangle = \frac{2}{\sigma_{tot}^{hN}}\int d^2s\ \mathrm{Re}\,\Gamma^{hN}(s)\left|\Psi_d(s)\right|^2 \approx \left|\Psi_d(0)\right|^2\ , \tag{85}$$

where we neglected the elastic slope B_{NN} compared to the nuclear radius squared. For the parton distribution functions in a nucleon we use the leading order GRV parametrization [56].

We calculated this ratio using the computer code for the Cronin effect developed in [4][7], and the deuteron wave function $\Psi_d(\vec{r}_T)$ described in Appendix B.

The results for $R_{d/p}(p_T)$ are depicted in Fig. 11. Indeed, the Cronin enhancement is only

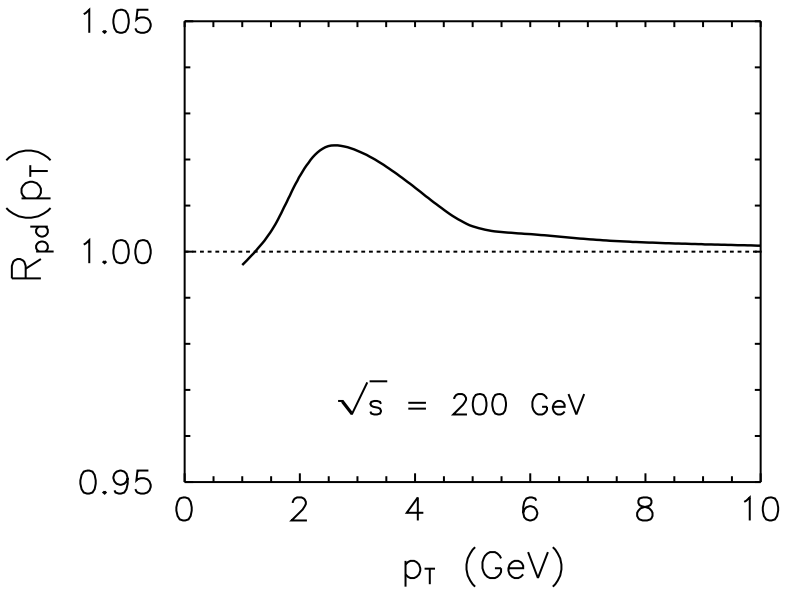

Figure 11: *Cronin ratio $R_{pd}(p_T)$ calculated at $\sqrt{s} = 200\,GeV$ using the formalism developed in [4].*

2%, and can be neglected comparing $d - Au$ data with predictions done for $p - Au$.

8 Summary and conclusions

The main observations and results of this paper are:

[7] I am thankful to Jan Nemchik who performed this calculation for *pd* collisions.

- The current normalization of inclusive high-p_T cross section in deuteron-gold collisions measured at RHIC is based on Glauber model calculations of the inelastic dAu cross section which is subject to Gribov's inelastic shadowing corrections. Importance of these corrections is not debatable, they have solid theoretical ground and are confirmed by precise measurements [10,19] (see Fig. 1). These corrections, Eq. (26), have negative sign, i.e. make nuclear medium more transparent, and they rise with energy.

- First of all, the Glauber calculations must be improved. The inelastic NN cross section used as an input should be corrected for diffraction. For experiments insensitive to diffraction (PHENIX, PHOBOS) the cross section should be reduced from $\sigma_{in}^{NN} = 42\,\mathrm{mb}$ down to $\tilde{\sigma}_{in}^{NN} \approx 30\,\mathrm{mb}$. On the contrary, if an experimental trigger detects diffraction (STAR) this cross section should be increased up to $\sigma_{tot}^{NN} = 51\,\mathrm{mb}$. This modification results in a correction factor K_{Gl} presented in Table 1.

- There are two types of inelastic shadowing corrections. One corresponds to diffractive excitation of the valence quark skeleton, or nucleonic resonances, and is related to the $I\!P I\!P I\!R$ triple-Regge graph. We calculated this correction, Eqs. (42), (61), (64), using the light-cone dipole representation which effectively sums up all orders of multiple interactions.

- Another type of inelastic shadowing is related to diffractive gluon bremsstrahlung, or to the soft limit of gluon shadowing in nuclei related to the $I\!P I\!P I\!P$ triple-Pomeron diffraction. We performed calculations in Sect. 6 using the solution for the Green function, Eq. (74), describing propagation of a glue-glue dipole through nuclear medium and found a rather weak gluon shadowing for gold, about 20%. At the same time, other models predict much stronger gluon shadowing ranging up to corrections of 70% (Sect. 6.2).

- Altogether, we expect a reduction of inelastic dAu cross section compared to what was used for normalization of high-p_T data at RHIC. We conclude that the published data should be corrected by factor K which is about 0.8 for PHENIX and about 0.9 for STAR (see Table 1). The renormalized data for pions do not possess any more the Cronin enhancement. This correction factor might be even smaller, down to 0.65 if to use a stronger gluon shadowing predicted by other models.

- One should admit that current data for high-p_T hadron production in dAu collisions at RHIC cannot exclude in a model independent way the possibility of initial state suppression suggested in [6], although that would contradict the author's personal viewpoints.

- Probably the only way to settle this uncertainty is a direct measurement of either the cross section of high-p_T pion production in dAu collisions, or the inelastic dAu cross sections at RHIC.

- A very sensitive test of models for inelastic shadowing offer tagged events with a spectator nucleon. In situation when direct measurement of dAu inelastic cross section

is difficult, this might be a way to restrict models and narrow the band of theoretical uncertainty. The relative fraction of these events 20% measured in [2] create apparent problems for models with strong gluon shadowing which predict a much larger fraction. Even with our weak shadowing this fraction ranges between 23% and 26%. However, one should make it sure that the detected neutrons are really spectators, what is not the case currently (see discussion in Sect. 3).

- We found a beautiful quantum-mechanical effect: the nucleus acts like a lens focusing spectators. In spite of the naive anticipation that nucleons which escaped interaction retain their primordial Fermi momentum distribution, there is a strong narrowing effect substantially reducing the transverse momenta of the spectators. Besides, the distribution acquires the typical diffractive maxima and minima (see Figs. 5 - 6).

Acknowledgments: This notes were written during visiting at Columbia University and I am thankful to Miklos Gyulassy and Alberto Accardi for hospitality and many inspiring discussions. I have also been much benefited from discussions with Barbara Jacak, Peter Levai, Ziwei Lin, Sasha Milov, Denes Molnar, Sergei Voloshin and other participants of the workshop, as well as with Peter Braun-Munzinger, Claudio Ciofi, Alexei Denisov, Jörg Hüfner, Yuri Ivanov, Berndt Müller, Andreas Schäfer, Mike Tannenbaum, and Xin-Nian Wang. My special thanks go to Yuri Ivanov and Irina Potashnikova for their kind assistance with numerical calculations. This work is supported by the grant from the Gesellschaft für Schwerionenforschung Darmstadt (GSI), grant No. GSI-OR-SCH, and by the grant INTAS-97-OPEN-31696.

9 Appendix

A Glauber model glossary

The hA elastic amplitude at impact parameter b has the eikonal form,

$$\Gamma^{hA}(\vec{b};\{\vec{s}_j,z_j\}) = 1-\prod_{k=1}^{A}\left[1-\Gamma^{hN}(\vec{b}-\vec{s}_k)\right] \ , \tag{A.1}$$

where $\{\vec{s}_j,z_j\}$ denote the coordinates of the target nucleon N_j. $i\Gamma^{hN}$ is the elastic scattering amplitude on a nucleon normalized as,

$$\begin{aligned}\sigma_{tot}^{hN} &= 2\int d^2b\ \mathrm{Re}\,\Gamma^{hN}(b);\\ \sigma_{el}^{hN} &= \int d^2b\,|\Gamma^{hN}(b)|^2\ .\end{aligned} \tag{A.2}$$

A.1 Heavy nuclei

In the approximation of single particle nuclear density one can calculate a matrix element between the nuclear ground states.

$$\left\langle 0\Big|\Gamma^{hA}(\vec{b};\{\vec{s}_j,z_j\})\Big|0\right\rangle = 1-\left[1-\frac{1}{A}\int d^2s\,\Gamma^{hN}(s)\int\limits_{-\infty}^{\infty}dz\,\rho_A(\vec{b}-\vec{s},z)\right]^A\ , \tag{A.3}$$

where

$$\rho_A(\vec{b}_1,z_1)=\int\prod_{i=2}^{A}d^3r_i\,|\Psi_A(\{\vec{r}_j\})|^2\ , \tag{A.4}$$

is the nuclear single particle density.

Total cross section. The result Eq. (A.3) is related via unitarity to the total hA cross section,

$$\begin{aligned}\sigma_{tot}^{hA} &= 2\,\mathrm{Re}\int d^2b\left\{1-\left[1-\frac{1}{A}\int d^2s\,\Gamma^{hN}(s)\,T_A(\vec{b}-\vec{s})\right]^A\right\}\\ &\approx 2\int d^2b\left\{1-\exp\left[-\frac{1}{2}\,\sigma_{tot}^{hN}\,(1-i\rho_{pp})\,T_A^h(b)\right]\right\}\ ,\end{aligned} \tag{A.5}$$

where ρ_{pp} is the ratio of the real to imaginary parts of the forward pp elastic amplitude;

$$T_A^h(b)=\frac{2}{\sigma_{tot}^{hN}}\int d^2s\ \mathrm{Re}\,\Gamma^{hN}(s)\,T_A(\vec{b}-\vec{s})\ ; \tag{A.6}$$

and

$$T_A(b)=\int_{-\infty}^{\infty}dz\,\rho_A(b,z)\ , \tag{A.7}$$

is the nuclear thickness function. We use exponential form of $\Gamma^{hN}(s)$ throughout the paper,

$$\mathrm{Re}\,\Gamma^{hN}(s)=\frac{\sigma_{tot}^{hN}}{4\pi B_{hN}}\ \exp\left(\frac{-s^2}{2B_{hN}}\right)\ , \tag{A.8}$$

where B_{hN} is the slope of the differential hN elastic cross section. Note that the accuracy of the optical approximation in (A.5) is quite high for gold, $\sim 10^{-3}$, so we use it throughout the paper. We also neglect the real part of the elastic amplitude in what follows, since it gives a vanishing correction $\sim\rho_{pp}^2/A^{2/3}$.

Elastic cross section. As far as the partial elastic amplitude is known, the elastic cross section reads,

$$\sigma_{el}^{hA}=\int d^2b\left|1-\exp\left[-\frac{1}{2}\,\sigma_{tot}^{hN}\,T_A^h(b)\right]\right|^2\ . \tag{A.9}$$

Total inelastic cross section. Apparently it is given by the difference between the total and elastic cross sections,

$$\sigma_{in}^{hA}=\sigma_{tot}^{hA}-\sigma_{el}^{hA}=\int d^2b\left\{1-\exp\left[-\sigma_{tot}^{hN}\,T_A^h(b)\right]\right\}\ . \tag{A.10}$$

This includes all inelastic channels when either the hadron or the nucleus (or both) are broken up.

Quasielastic cross section. As a result of the collision the nucleus can be excited to a state $|F\rangle$. Summing over final states of the nucleus and applying the condition of completeness, one gets the quasielastic cross section,

$$\begin{aligned}\sigma_{qel}^{hA} &= \sum_F \int d^2b \, \left[\left\langle 0 \left| \Gamma^{hA}(b) \right| F \right\rangle^\dagger \left\langle F \left| \Gamma^{hA}(b) \right| 0 \right\rangle - \left| \left\langle 0 \left| \Gamma^{hA}(b) \right| 0 \right\rangle \right|^2 \right] \\ &= \int d^2b \, \left[\left\langle 0 \left| \left| \Gamma^{hA}(b) \right|^2 \right| 0 \right\rangle - \left| \left\langle 0 \left| \Gamma^{hA}(b) \right| 0 \right\rangle \right|^2 \right] \ . \end{aligned} \tag{A.11}$$

Here we extracted the cross section of elastic scattering when the nucleus remains intact.

Then in the fist term of this expression we make use of the relation,

$$\mathrm{Re} \int d^2s \, \frac{T_A^h(\vec{b}-\vec{s})}{A} \left\{ 1 - 2\Gamma^{hN}(s) + \left[\Gamma^{hN}(s) \right]^2 \right\} \approx 1 - \frac{1}{A} \, T_A^h(b) (\sigma_{tot}^{hN} - \sigma_{el}^{hN}) \ , \tag{A.12}$$

and arrive at,

$$\sigma_{qel}^{hA} = \int d^2b \, \left\{ \exp\left[-\sigma_{in}^{hN} \, T_A^h(b) \right] - \exp\left[-\sigma_{tot}^{hN} \, T_A^h(b) \right] \right\} \ . \tag{A.13}$$

Inelastic nondiffractive cross section. If one is interested in the fraction of the total inelastic cross section (A.10) which covers only reactions with production of new particles, one should exclude the nucleus break up to nucleons and nuclear fragments. That is the quasielastic cross section, Eq. (A.13),

$$\sigma_{prod}^{hA} = \int d^2b \, \left\{ 1 - \exp\left[-\sigma_{in}^{hN} \, T_A^h(b) \right] \right\} \ . \tag{A.14}$$

This additional subtraction makes sense only for experiments which miss the non-production break up of the nucleus. If, however, all inelastic events are detected, including diffractive (production and non-production channels) excitations of the nucleus (check with [2]) one should rely on Eq. (A.10) for the inelastic nuclear cross section.

Diffractive cross section. One needs to know this cross section in order to subtract it also from the inelastic cross section, since diffractive events escape registration at $p(d)A$ collisions at SPS and RHIC. The Glauber approximation is valid only for a single channel problem. One can extend it to include diffraction properly introducing phase shifts due to longitudinal momentum transfer. However, one needs to know the cross section of interaction of the produced diffractive excitation with nucleons. This goes beyond the reach of the Glauber model, and instead of further ad hoc development of the model, we solve this problem within the eigenstate method in Section 4.2.

A.2 Proton-deuteron collisions

Apparently, Eq. (A.5) should not be applied to light nuclei, in particular to a deuteron. Instead one should use,

$$\sigma_{tot}^{pd} = 2\sigma_{tot}^{NN} + \Delta\sigma_{tot}^{pd} \ , \tag{A.15}$$

where

$$\Delta\sigma_{tot}^{pd} = -2\int d^2b \int d^2r_T \; |\Psi_d(r_T)|^2 \; \Gamma^{hN}(\vec{b}+\vec{r}_T/2)\,\Gamma^{hN}(\vec{b}-\vec{r}_T/2) \; . \tag{A.16}$$

One can switch via Fourier transform to momentum representation in each of these three factors and perform integration over $\vec{r}_T$ and $\vec{b}$. The result has a form of a one-dimensional integral [16],

$$\Delta\sigma_{tot}^{pd} = -\frac{2}{\pi}\int d^2q_T \, F_d(4q_T^2)\,\frac{d\sigma_{el}^{NN}}{dq_T^2} \; , \tag{A.17}$$

where $F_d(q^2)$ is the charge formfactor of the deuteron. We neglected the correction $\sim 10^{-3}$ due to the nonzero real part of the forward NN amplitude. Note that $\vec{s}$ in (A.17) is the deuteron diameter, rather than the radius. This is why the formfactor argument is $4q_T^2$.

We use parametrization of the deuteron formfactor from [24],

$$F_d(q_T^2) = 0.55\, e^{-\alpha q_T^2} + 0.45\, e^{-\beta q_T^2} \; , \tag{A.18}$$

and $\alpha = 19.66\,\mathrm{GeV}^{-2}$, $\beta = 4.67\,\mathrm{GeV}^{-2}$.

Using $\sigma_{tot}^{NN} = 51\,\mathrm{mb}$ at $\sqrt{s} = 200\,\mathrm{GeV}$, and the elastic slope $B_{NN} = 14\,\mathrm{GeV}^{-2}$ we found the total pd cross section, $\sigma_{tot}^{pd} = 97\,\mathrm{mb}$ with Glauber correction $\Delta_{Gl}^{pd} = -5\,\mathrm{mb}$. Since at this point a correct proton-deuteron cross section is needed, we have to go beyond the Glauber approximation and add the inelastic correction considered in Sect. 4. We show that it is equivalent to adding the differential cross section of single diffraction, $pN \to XN$, to the elastic one in (A.17). This increases the value of the shadowing correction by 1.75 mb. Finally, we arrive at the cross sections,

$$\begin{aligned} \sigma_{tot}^{pd} &= 95.15\,\mathrm{mb} \\ \sigma_{in}^{pd} &= \sigma_{tot}^{pd} - \frac{(\sigma_{tot}^{pd})^2}{16\pi\, B_{pd}} = 84.9\,\mathrm{mb} \; . \end{aligned} \tag{A.19}$$

Interesting, the inelastic cross section is not affected by the Glauber correction, it is even slightly larger that the sum of two inelastic NN cross sections. The slope from the differential elastic pd cross section was measured and fitted in [62],

$$\frac{d\sigma_{el}^{pd}}{dt} = \frac{(\sigma_{tot}^{pd})^2}{16\pi}\; e^{B_{pd}t + C_{pd}t^2} \; , \tag{A.20}$$

where

$$B_{pd} = b_0 + b_1 \ln s_{pd} \; , \tag{A.21}$$

with parameters $b_0 = 32.8 \pm 0.6$ (GeV^2) and $b_1 = 1.01 \pm 0.09$ (GeV^2). Parameter $C_{pd} = 54.0 \pm 0.9$ (GeV^-2) was found to be energy independent. At the energy of RHIC $B_{pd} = 44.1\,\mathrm{GeV}^{-2}$, and we use this value in (A.19).

The inelastic cross section Eq. (A.19) contains inelastic diffractive channels like quasielastic break up of the deuteron, $pd \to ppn$, and excitation of the nucleons $pd \to Xd$, $pd \to pY$, and $pd \to XY$. For the experiments insensitive to diffraction (PHENIX,PHOBOS) those channels must be subtracted.

B Deuteron wave function at rest and Lorentz boosted

To perform calculations for interaction of a high energy deuteron, one should not use the three-dimensional deuteron wave function, but needs to know the light-cone deuteron wave function expressed in Lorentz invariant variables, the transverse $n-p$ separation $\vec{r}_T$ and the light-cone fraction $\alpha = p_n^+/p_d^+$ of the deuteron momentum carried by a nucleon. One cannot get this wave function by a simple Lorentz boost from the rest frame of the deuteron, where the 3-dimensional wave function is supposed to be known, to the infinite momentum frame. Deuteron is not a classical system, under a Lorentz boost it acquire new constituents which are quantum fluctuations. These constituents build up higher Fock components. This makes the procedure of Lorentz boost extremely complicated. There is, however, a practical recipe suggested in [63] and widely accepted. To the best knowledge of the author, it works rather well for nonrelativistic systems (nuclei [64], heavy quarkonia [65], etc.)

The idea is straightforward, first, to express the deuteron wave function in momentum representation,

$$\psi_d(\vec{q}) = \frac{1}{(2\pi)^3}\int d^3r\, e^{i\vec{q}\cdot\vec{r}}\,\psi_d(\vec{r}) \ , \tag{B.1}$$

via the light-cone variables in the rest frame of the deuteron. To do it one should connect the three-dimensional momentum squared with the effective mass of the $c\bar{c}$ pair, $q^2 = M^2/4 - m_N^2$, expressed in terms of light-cone variables

$$M^2(\alpha, q_T) = \frac{q_T^2 + m_N^2}{\alpha(1-\alpha)} \ . \tag{B.2}$$

In order to change integration variable q_L to the light-cone α one uses their relation, $q_L = (\alpha - 1/2)M(q_T, \alpha)$, and get a Jacobian which can be attributed to the definition of the light-cone wave function,

$$\psi(\vec{q}) \Rightarrow \sqrt{2}\,\frac{(q^2+m_N^2)^{3/4}}{(q_T^2+m_N^2)^{1/2}}\cdot\psi(\alpha,\vec{q}_T) \equiv \Psi(\alpha,\vec{q}_T) \ . \tag{B.3}$$

Applying this procedure to the S and D-wave radial wave functions one gets,

$$\begin{aligned} \frac{u(\vec{r})}{r} &\Rightarrow U(\vec{r}_T,\alpha) \ ; \\ \frac{w(\vec{r})}{r} &\Rightarrow W(\vec{r}_T,\alpha) \ . \end{aligned} \tag{B.4}$$

This dependence on α is important for exclusive final states, for instance deuteron dissociation to nucleons with definite longitudinal momenta. However, for most of applications in this paper we need to know the r_T-retribution integrated over α,

$$|\Psi_d(r_T)|^2 = \int\limits_0^1 d\alpha \left[U^2(r_T,\alpha) + W^2(r_T,\alpha)\right] \ , \tag{B.5}$$

The result of this is identical to the simple integration over longitudinal variable in the rest frame of the nucleus,

$$|\Psi_d(r_T)|^2 = \int\limits_{-\infty}^{\infty} dr_L\ \frac{u^2(r)+w^2(r)}{r^2} \ . \tag{B.6}$$

We use the contemporary deuteron wave functions which employ the Nijmegen-93 potential [66][8].

References

[1] PHENIX Collaboration, K. Adcox et al., *Absence of Suppression in Particle Production at Large Transverse Momentum in* $\sqrt{s_{NN}} = 200\,GeV$ *d+Au Collisions*, nucl-ex/0306021.

[2] STAR Collaboration, J. Adams et al. *Transverse momentum and collision energy dependence of high* p_T *hadron suppression in Au+Au collisions at ultrarelativistic energies*, nucl-ex/0305015.

[3] PHOBOS Collaboration, B.B. Back et al. *Centrality dependence of charged hadron transverse momentum spectra in d+Au collisions at* $\sqrt{s_{NN}} = 200\,GeV$, nucl-ex/0306025.

[4] B.Z. Kopeliovich, J. Nemchik, A. Schaefer, A.V. Tarasov, Phys. Rev. Lett. **88** (2002) 232303.

[5] I. Vitev, M. Gyulassy, Phys.Rev.Lett. **89** (2002) 252301.

[6] D. Kharzeev, E. Levin, L. McLerran, Phys.Lett. B561 (2003) 93.

[7] D. Antreasyan et al., Phys. Rev. **D19**, 764 (1979)

[8] A.V. Abramovsky, V.N. Gribov and O.V. Kancheli, Yad. Fiz. **18**, 595 (1973).

[9] V.N. Gribov, Sov. Phys. JETP **56** (1968) 892.

[10] P.V.R. Murthy et al., Nucl. Phys. **B92**, 269 (1975).

[11] B.Z. Kopeliovich, A. Schäfer and A.V. Tarasov, Phys. Rev. **D62** (2000) 054022

[12] K. Goulianos, J. Montanha, Phys. Rev. **D59**, 114017 (1999)

[13] CDF Collaboration, T. Affolder et al., Phys. Rev. Lett. **87**, 141802 (1991).

[14] Barbara V. Jacak, private communication.

[15] Michael J. Tannenbaum, private communication.

[16] R.J. Glauber, Phys. Rev. **100** (1955) 42

[17] V. Karmanov and L.A. Kondratyuk, Sov. Phys. JETP Lett. **18** (1973) 266.

[18] B.Z. Kopeliovich and J. Nemchik, Phys. Lett. **B368**, 187 (1996)

[8] I am grateful to Miklos Gyulassy for suggesting this and providing relevant data.

[19] A. Gsponer et al., Phys. Rev. Lett. **42**, 9 (1979).

[20] B.Z. Kopeliovich, J. Raufeisen and A.V. Tarasov, Phys. Lett. **B440** (1998) 151; J. Raufeisen, A.V. Tarasov and O.O. Voskresenskaya, Eur. Phys. J. A **5** (1999) 173.

[21] B.Z. Kopeliovich, J. Raufeisen and A.V. Tarasov, Phys. Rev. **C62** (2000) 035204.

[22] B.Z. Kopeliovich and L.I. Lapidus, Sov. Phys. JETP Lett. **28** (1978) 664

[23] J. Pumplin and M. Ross, Phys. Rev. Lett. **21**, 1778 (1968).

[24] V.V. Anisovich, P.E. Volkovitsky, and L.G. Dakhno, Phys. Lett. **42B**, 224 (1972).

[25] E. Feinberg and I.Ya. Pomeranchuk, Nuovo. Cimento. Suppl. **3** (1956) 652

[26] M.L. Good and W.D. Walker, Phys. Rev. **120** (1960) 1857

[27] H.I. Miettinen and J. Pumplin, Phys. Rev.**D18** (1978) 1696

[28] A.B. Zamolodchikov, B.Z. Kopeliovich and L.I. Lapidus, Sov. Phys. JETP Lett. **33** (1981) 612

[29] B.Z. Kopeliovich and B.G. Zakharov, Phys. Rev. **D44** (1991) 3466.

[30] M. Anselmino, E. Predazzi, S. Ekelin, S. Fredriksson, and D.B. Lichtenberg, Rev. Mod. Phys. **65** (1993) 1199.

[31] B.Z. Kopeliovich and B.G. Zakharov, Phys. Lett. **211B**, 221 (1988); Sov. J. Nucl. Phys. **48**, 136 (1988); Sov. Phys. Particles and Nuclei, **22**, 140 (1991).

[32] B. Povh and J. Hüfner, Phys. Rev. Lett. **58**, 1612 (1987).

[33] K. Golec-Biernat and M. Wüsthoff, Phys. Rev. D**59** (1999) 014017.

[34] A.M. Stasto, K. Golec-Biernat, J. Kwiecinski, Phys. Rev. Lett. **86**, 596 (2001).

[35] S. Amendolia et al., Nucl. Phys. **B277** (1986) 186

[36] L.D. Landau and I.Ya. Pomeranchuk, *ZhETF* **24**, 505 (1953);
L.D. Landau, I.Ya. Pomeranchuk, *Doklady AN SSSR* **92**, 735 (1953);
E.L. Feinberg and I.Ya. Pomeranchuk, *Doklady AN SSSR* **93**, 439 (1953);
I.Ya. Pomeranchuk, *Doklady AN SSSR* **96**, 265 (1954);
I.Ya. Pomeranchuk, *Doklady AN SSSR* **96**, 481 (1954):
E.L. Feinberg, I.Ya. Pomeranchuk, *Nuovo Cim. Suppl.* **4**, 652 (1956).

[37] A.B. Migdal, Phys. Rev. **103**, 1811 (1956).

[38] B. Z. Kopeliovich, proc. of the workshop *Dynamical Properties of Hadrons in Nuclear Matter,* Hirschegg, January 16 – 21, 1995, ed. by H. Feldmeyer and W. Nörenberg, Darmstadt, 1995, p. 102 (hep-ph/9609385).

[39] T. Schäfer, E.V. Shuryak, Rev. Mod. Phys. **70**, 323 (1998).

[40] M. D'Elia, A. Di Giacomo and E. Meggiolaro, Phys. Lett. **B408**, 315 (1997).

[41] B.Z. Kopeliovich, I.K. Potashnikova, B. Povh, E. Predazzi, Phys. Rev. Lett. **85**, 507 (2000); Phys. Rev. **D63**, 0540012001 (2002).

[42] B.Z. Kopeliovich, A. Schäfer and A.V. Tarasov, Phys. Rev. **C59**,1609 (1999).

[43] B.Z. Kopeliovich, J. Nemchik, A. Schaefer, A.V. Tarasov,, Phys. Rev. **C65**, 035201 (2002).

[44] B.Z. Kopeliovich, J. Raufeisen, A.V. Tarasov, M.B. Johnson, Phys. Rev. **C67** (2003) 014903.

[45] L.V. Gribov, E.M. Levin and M.G. Ryskin, Nucl. Phys. **B188** (1981) 555; Phys. Rep. **100** (1983) 1.

[46] I.I. Balitsky, Nucl. Phys. **B463**, 99 (1996); Yu.V. Kovchegov, Phys. Rev. **D60**, 034008 (1999).

[47] L. Frankfurt and M. Strikman, Eur. Phys. J. **A5**, 293 (1999).

[48] L. Frankfurt, V. Guzey, M. McDermott, M. Strikman, JHEP **0202**, 027 (2002).

[49] Z. Huang, H.J. Lu and I. Sarcevic, Nucl. Phys. **A637**, 79 (1998).

[50] B. Blättel et al., Phys. Rev. Lett. **70**, 896 (1993).

[51] G. Orwell, *Animal Farm*, Signet Classic, New American Library, New York, 1996.

[52] S. y Li and X.-N. Wang, Phys. Lett. **B 575**, 85 (2002).

[53] L. Alvero, J.C. Collins and J.J. Whitmore, Phys. Rev. **D59** (1999) 074022; hep-ph/9806340.

[54] E.M. Levin, private communication.

[55] L. McLerran and R. Venugopalan, Phys. Rev. D **49**, 2233 (1994); **49**, 3352 (1994); **49**, 2225 (1994).

[56] M. Gluck, E. Reya, and A. Vogt, Z. Phys. C **67**, 433 (1995).

[57] G.T. Bodwin, S.J. Brodsky, and G.P. Lepage, Phys. Rev. D **39**, 3287 (1989).

[58] X.-N. Wang, Phys.Rev. **C61**, 064910 (2000).

[59] I. Vitev, Phys. Lett. **B562**, 36 (2003).

[60] J. Dolejši, J. Hüfner and B.Z. Kopeliovich, Phys.Lett. **B312**, 235 (1993).

[61] M.B. Johnson, B.Z. Kopeliovich, and A.V. Tarasov, Phys. Rev. **C63**, 035203 (2001).

[62] Yu. Akimov et al., Phys. Rev. D 12, 33993413 (1975); ibid D15, 2040(E) (1977).

[63] M.V. Terent'ev, Sov. J. Nucl. Phys., **24**, 106 (1976).

[64] L. Frankfurt and M. Strikman, Phys. Rept. **76**, 217 (1981); *ibid* **160**, 235 (1988).

[65] J. Hüfner, Yu.P. Ivanov, B.Z. Kopeliovich, A.V. Tarasov, Phys. Rev. **D62**, 094022 (2000); Phys. Rev. **C66**, 024903 (2002).

[66] V.G.J. Stoks, R.A.M. Klomp, C.P.F. Terheggen and J.J. de Swart, Phys. Rev. **C 49**, 2950 (1994).